NAVAL POSTGRADUATE SCHOOL

MONTEREY, CALIFORNIA

THESIS

STUDY OF COMPOSITE INTERFACE STRENGTH AND CRACK GROWTH MONITORING USING CARBON NANOTUBES

by

Mollie A. Bily

September 2009

Thesis Advisor:	Young W. Kwon
Second Reader:	Randall D. Pollak

Approved for public release; distribution is unlimited

REPORT DOCUMENTATION PAGE			Form Approved OMB No. 0704-0188
Public reporting burden for this collection of information is estimated to average 1 hour per response, including the time for reviewing instruction, searching existing data sources, gathering and maintaining the data needed, and completing and reviewing the collection of information. Send comments regarding this burden estimate or any other aspect of this collection of information, including suggestions for reducing this burden, to Washington headquarters Services, Directorate for Information Operations and Reports, 1215 Jefferson Davis Highway, Suite 1204, Arlington, VA 22202-4302, and to the Office of Management and Budget, Paperwork Reduction Project (0704-0188) Washington DC 20503.			
1. AGENCY USE ONLY ***(Leave blank)***	**2. REPORT DATE** September 2009	**3. REPORT TYPE AND DATES COVERED** Master's Thesis	
4. TITLE AND SUBTITLE Study of Composite Interface Strength and Crack Growth Monitoring Using Carbon Nanotubes		**5. FUNDING NUMBERS**	
6. AUTHOR(S) Mollie A. Bily			
7. PERFORMING ORGANIZATION NAME(S) AND ADDRESS(ES) Naval Postgraduate School Monterey, CA 93943-5000		**8. PERFORMING ORGANIZATION REPORT NUMBER**	
9. SPONSORING /MONITORING AGENCY NAME(S) AND ADDRESS(ES) N/A		**10. SPONSORING/MONITORING AGENCY REPORT NUMBER**	
11. SUPPLEMENTARY NOTES The views expressed in this thesis are those of the author and do not reflect the official policy or position of the Department of Defense or the U.S. Government.			
12a. DISTRIBUTION / AVAILABILITY STATEMENT Approved for public release; distribution is unlimited		**12b. DISTRIBUTION CODE**	

13. ABSTRACT (maximum 200 words)

Interface strength of woven fabric composite layers was studied using Mode II fracture strength testing. Both carbon fiber and glass fiber composites were used with the vinyl ester resin. First, the single-step cured (i.e., co-cured) composite interface strength was compared to that of the two-step cured interface as used in the scarf joint technique. The test results showed that the two-step cured interface was as strong as the co-cured interface, and the former had even higher fracture toughness than the latter. The second study applied carbon nanotubes to the composite interface using the two-step curing technique. Mode II fracture testing was performed for the interface containing carbon nanotubes. The results indicated great improvement of the interface fracture toughness due to carbon nanotubes. Finally, a study was conducted to detect interface crack growth using the carbon nanotubes introduced at the interface. Because carbon nanotubes have high electric conductivity, the electric resistance was measured though the interface. As the interface crack grew under a loading, there was a gradual increase of electric resistance. As a result, the change of electric resistance in terms of crack length change was determined. The study showed that using carbon nanotubes at a critical composite interface would not only strengthen its fracture toughness but also detect crack growth.

14. SUBJECT TERMS Carbon Nanotubes, CNTs, Carbon Fiber Composite, Fiberglass Composite, Crack Propagation, Mode II, Health Monitoring, Resistance Testing			**15. NUMBER OF PAGES** 93
			16. PRICE CODE
17. SECURITY CLASSIFICATION OF REPORT Unclassified	**18. SECURITY CLASSIFICATION OF THIS PAGE** Unclassified	**19. SECURITY CLASSIFICATION OF ABSTRACT** Unclassified	**20. LIMITATION OF ABSTRACT** UU

NSN 7540-01-280-5500

Standard Form 298 (Rev. 2-89)
Prescribed by ANSI Std. 239-18

THIS PAGE INTENTIONALLY LEFT BLANK

Approved for public release; distribution is unlimited

STUDY OF COMPOSITE INTERFACE STRENGTH AND CRACK GROWTH MONITORING USING CARBON NANOTUBES

Mollie A. Bily
Lieutenant, United States Navy
B.S., United States Naval Academy, 2003

Submitted in partial fulfillment of the
requirements for the degree of

MASTER OF SCIENCE IN MECHANICAL ENGINEERING

from the

NAVAL POSTGRADUATE SCHOOL
September 2009

Author: Mollie A. Bily

Approved by: Young W. Kwon
Thesis Advisor

Randall D. Pollak
Second Reader

Knox T. Millsaps
Chairman, Department of Mechanical and Astronautical Engineering

THIS PAGE INTENTIONALLY LEFT BLANK

ABSTRACT

Interface strength of woven fabric composite layers was studied using Mode II fracture strength testing. Both carbon fiber and glass fiber composites were used with the vinyl ester resin. First, the single-step cured (i.e., co-cured) composite interface strength was compared to that of the two-step cured interface as used in the scarf joint technique. The test results showed that the two-step cured interface was as strong as the co-cured interface, and the former had even higher fracture toughness than the latter. The second study applied carbon nanotubes to the composite interface using the two-step curing technique. Mode II fracture testing was performed for the interface containing carbon nanotubes. The results indicated great improvement of the interface fracture toughness due to carbon nanotubes. Finally, a study was conducted to detect interface crack growth using the carbon nanotubes introduced at the interface. Because carbon nanotubes have high electric conductivity, the electric resistance was measured though the interface. As the interface crack grew under a loading, there was a gradual increase of electric resistance. As a result, the change of electric resistance in terms of crack length change was determined. The study showed that using carbon nanotubes at a critical composite interface would not only strengthen its fracture toughness but also detect crack growth.

THIS PAGE INTENTIONALLY LEFT BLANK

TABLE OF CONTENTS

LIST OF FIGURES

ACKNOWLEDGMENTS

I would like to thank Dr. Young Kwon for his mentorship and patience during the course of this research and throughout my graduate studies.

Major Randall Pollak, USAF, is also appreciated for providing guidance particularly in the area of Carbon Nanotube Non-Destructive Testing.

Many thanks to Tom Christen and Chanman Park for their technical advice and for giving up their valuable time to help choose, set up, and take down test equipment.

Thanks to the Air Force Office of Scientific Research and the Naval Surface Warfare Center Carderock Division (NSWCCD) team for "Advanced Hull Materials & Structures Technology (AHM&ST)" who provided crucial funding and materials.

Thank you to Integrated Composites for use of their equipment during the course of my research.

Last, but certainly not least, I would like to thank my husband, John, for his support and patience throughout my entire time here at the Naval Postgraduate School.

THIS PAGE INTENTIONALLY LEFT BLANK

I. INTRODUCTION

A. BACKGROUND

In the past decade, composite structures have been in the forefront of structural research. In particular, the Department of Defense has looked at both carbon fiber and fiberglass composites for use in construction of ship superstructures, submarine sails, and structures of unmanned aircraft.[1] Many promising steps have been taken to ensure that composites are fully integrated into structural use. A recurring hindrance to successful integration of composite structures is that of critical areas of stress concentration, and their ability to withstand failure.

Carbon-Carbon bonds are one of the strongest of chemical bonds found in nature, and are the basis for the strength of carbon nanotubes. Carbon nanotubes (CNTs) are made of sp^2 hybridized carbon bonds, with each atom joined to three neighbors creating a hexagonal lattice structure like graphite.[2] The lattice structure forms a tube with a nano-sized diameter and can be several millimeters in length, as shown in Figure 1. The three main classifications of CNTs used in modern research are single-walled, double-walled, and multi-walled, meaning an inner cylinder lies within the outer cylinder as shown in Figure 2.[3] Although many strides have been made in the manufacturing of CNTs, they are still quite expensive. CNTs have an extremely high elastic modulus (greater than 1 TPa), high tensile strengths (up to 63 GPa), and are extremely lightweight, making them ideal for reinforcement of composite materials.[4]

---

[1] A.P. Mouritz, E. Gellert, P. Burchill, and K. Challis, "Review of Advanced Composite Structures for Naval Ships and Submarines," *Composite Structures* 53 (2001): 21–41.

[2] R. Saito and M. S. Dresselhaus, *Physical Properties of Carbon Nanotubes* (Imperial College Press, 1998), 11–12.

[3] William D. Callister, Jr., *Materials Science and Engineering: An Introduction* (New York: John Wiley and Sons, Inc, 2007), 433.

[4] P.J.F. Harris. "Carbon Nanotube Composites," *International Materials Review* 49 (2004): 31.

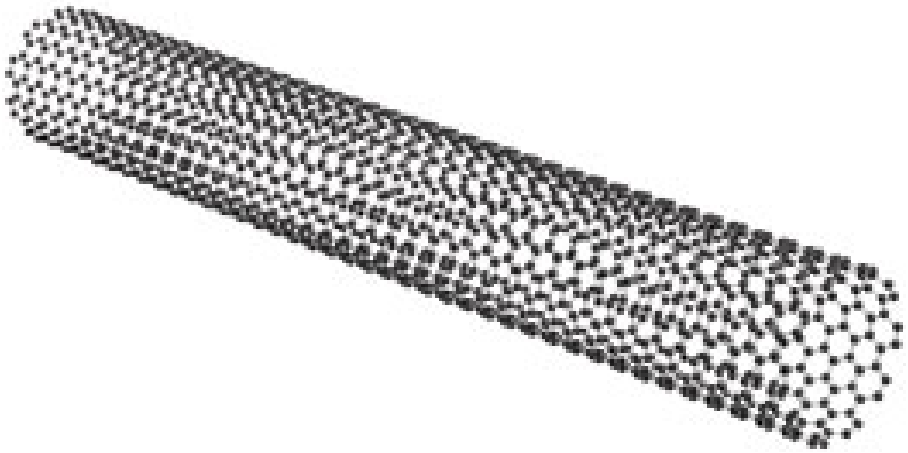

Figure 1. Single-Walled Carbon Nanotube[5]

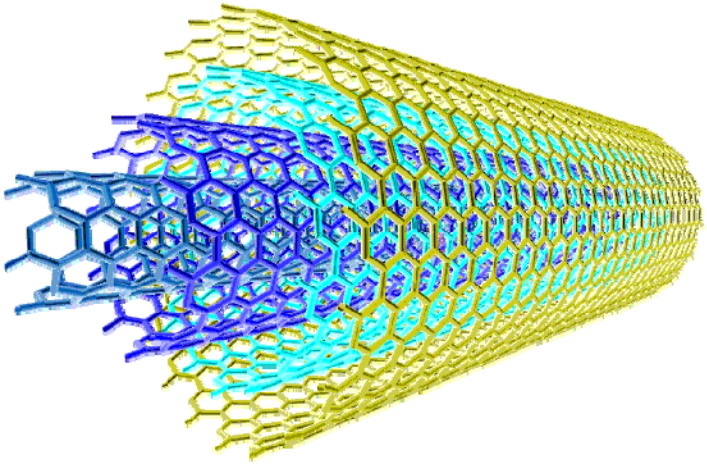

Figure 2. Multi-Walled Carbon Nanotube[6]

It has already been demonstrated that inclusion of CNTs in areas of high stress concentration can increase a material's ability to withstand stress at these critical areas.[7] However, a secondary benefit could be the use of CNTs to monitor composite materials

[5] The Venton Research Group. Development of Carbon Nanotube Modified Microelectrodes. n.d. http://www.faculty.virginia.edu/ventongroup/nanotube.html (accessed September 9, 2009)

[6] Live Journal. Definition of a Nanotube, March 12, 2009. http://fullerenes.livejournal.com/ (accessed September 9, 2009).

[7] Susan Faulkner, *Study of Composite Joint Strength with Carbon Nanotube Reinforcement*, Naval Postgraduate School, MS thesis, September 2008, 1–42.

to detect damage at interfaces. Compared to metals, the failure of composites is much more difficult to predict due to the accumulation of damage ultimately leading to failure.[8] Since failure is often difficult to predict, employing a network of CNTs at a critical juncture would provide a dual purpose for their inclusion in the composite material. Composite materials would be strengthened, while simultaneously detecting interfacial damage.

B. LITERAT URE REVIEW

Many different studies have been conducted to determine the feasibility of damage detection in composite materials through the use of CNTs. During one study a CNT polymer material was used to manufacture a piezoresistive strain sensor for structural health monitoring. This sensor proved to have a linear symmetric strain response under static and dynamic loading, however the CNTs were only included within the sensor itself.[9] One similar study conducted showed that multidirectional strains could be measured using an isotropic film of CNTs placed on a four point probe. This probe then could be moved around to different locations sensing a linear strain response in all locations.[10]

Another study, however, focused solely on the use of CNTs as a replacement for strain gauges. This study placed semi-conductive multiwall CNT-fiberglass–epoxy polymer composites under both tensile and cyclic loading to detect failure. It was shown that the multiwall CNTs were able to outperform regular strain gauges in sensing different types of failures. This was due to their ability to be interspersed within the composite and, as a result, be more sensitive to the changing stress fields around them.[11]

---

[8] I. Weber, and P. Schwartz, "Monitoring Bending Fatigue In Carbon-Fibre/Epoxy Composite Strands: A Comparison Between Mechanical and Resistance Techniques," *Composites Science and Technology* 61 (2001): 849–853.

[9] I. Kang, M.J. Schulz, J.H. Kim, V. Shanov, and D. Shi, "A Carbon Nanotube Strain Sensor for Structural Health Monitoring," *Smart Materials and Structures*, 15 (2006): 737–748.

[10] P. Dharap, Z. Li, S. Nagarajaiah, and Barrera, E.V, "Nanotube Film Based on Single-Wall Carbon Nanotubes for Strain Sensing," *Nanotechnology*, 15 (2004): 379–382.

[11] M. Nofar, S.V. Hoa, and M.D. Pugh, "Failure Detection and Monitoring in Polymer Matrix Composites Subjected to Static and Dynamic Loads Using Carbon Nanotube Networks," *Composites Science and Technology* (2009): 1–22.

Much work has been done to replace strain gauges, however limited research has been conducted based on crack propagation and local application of CNTs. In one study CNTs were first dispersed into a polymer matrix and then infiltrated into layers and bundles of conventional fibers. This created a percolating network which was then used as a sensor to detect the onset, nature and evolution of damage in advanced-polymer-based composites.[12] A similar study demonstrated that a network of CNTs throughout the composite material is an effective way to monitor fatigue-induced damage, as well as opportunities for damage repair.[13] Yet, another study showed that if a high aspect ratio could be maintained throughout the entire network of CNTs, they could be highly conductive within the structure allowing for damage detection.[14]

Each of these studies however, used a network of CNTs dispersed throughout the composite base material to achieve damage detection. These methods, although successful in the detection of damage, still may not address the interfacial damage mechanisms. In order to achieve this type of damage detection, a layer of CNTs percolated along the matrix surface is to be studied.

C. OBJECTIVES

The objective of this research is to advance the uses of CNTs within composite materials. Two main areas of research will be looked at and studied closely to further the implementation of CNTs as a local reinforcement.

Previous research showed that CNTs can increase the fracture toughness of the composite interface significantly; however, only one assembly mode, two-step cured, was used.[15] The first objective of this research is to determine the critical strain energy

---

[12] E.T. Thostenson and T. W. Chou, "Carbon Nanotube Networks: Sensing of Distributed Strain and Damage for Life Prediction and Self Healing," *Advanced Materials*, 18 (2006): 2837–2841.

[13] W. Zhang, V. Sakalkar, and N. Koratkar, "In Situ Health Monitoring and Repair In Composites Using Carbon Nanotube Additives," *Applied Physiscs Letters*, 91(2007).

[14] Tsu-Wei Chou and Erik T. Thosetenson. "Carbon Nanotube/Vinyl Ester Nanocomposites for in Situ Sensing," September 17-29, 2008. University of Maryland University College, Adelphia, MD. *Office of Naval Research Solid Mechanics Program Review Meeting: Marine Composites and Sandwich Structures:* 42–49.

[15] Faulkner, "Study of Composite Joint Strength with Carbon Nanotube Reinforcement," 15–42.

release rate, G, and crack propagation characteristics of carbon fiber vinyl ester resin composite during Mode II fractures for both single-step-cured (co-cured) and two-step cured composite sample sets. This ultimately will help determine the optimum way to manufacture composite materials with, and without, CNTs. If the data is the same, the methods can be interchanged and allow for more flexibility in the composite material assembly process.

Ideally, if CNTs are close enough together, as result of their conductive nature, they can conduct electrical current. The second objective of this research is to exploit this characteristic in order to determine if failure in a composite interface has occurred. Failure of a composite would occur if the material has deformed enough that the CNTs are no longer touching each other. In real-world applications, a procedure using current to test for failure would be beneficial to operational units, and would provide a method for real time monitoring, such as in situ health monitoring.

THIS PAGE INTENTIONALLY LEFT BLANK

II. COMPOSITE SAMPLE CONSTRUCTION

A. SAMPLE SPECIFICATION

Three different sample sets were constructed during this research. The first set consisted of two types of resin-only carbon composite coupons: one set of coupons being co-cured, and the other set being two-step cured. The second and third sample groups also consisted of two coupon types per sample set. One coupon group was fiber composite with resin-only, while the other fiber composite group was CNT-reinforced. The differences between the second and third sample sets were the type of base composite material used, being carbon and fiberglass, respectively.

Each sample set consisted of the same basic coupon construction, with varying parameters, and materials. All coupons had pre-existing cracks built into them in order to represent an area of high-stress concentration. The first sample set of coupons is exactly as depicted in Figure 3, whereas the second and third sample sets had stainless steel metal sheets built into each end to allow for current to run through the sample sets. For these two sample sets of coupons, the length of the crack was made sufficiently longer so that the extra width of the thin piece of metal did not affect the test results.

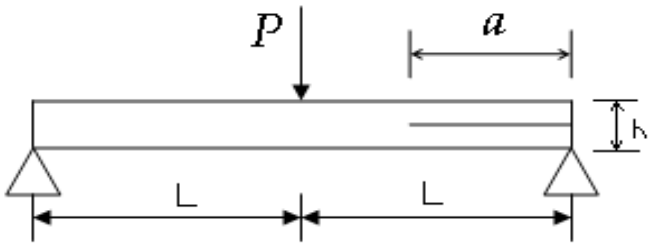

Figure 3. Sample Geometry[16].

Where: 2L = length
h = thickness
a = initial crack length

[16] Faulkner, "Study of Composite Joint Strength with Carbon Nanotube Reinforcement," 19.

B. MATERI ALS

Sample sets one and two were both constructed of TORAY T700CF carbon fiber weave with a vinyl-ester matrix whose base was DERAKANE 510–A. The third sample set also used DERKANE 510–A to create the base, but this time was made with bidirectional fiberglass woven roving. Typically, fiberglass woven roving is categorized by weight in ounces per square yard; for this research, 24-oz per square-yard woven roving was used. Both the carbon fiber weave and the fiberglass woven were chosen based on their current use in DoD structural projects.

In order to make the vinyl ester matrixes, the DERAKANE 510–A had to be cured and hardened. The hardening chemicals used for this process are Methyl Ethyl Ketone Peroxide (MEKP) and Cobalt Naphthenate (CoNap). MEKP was used to initiate the chemical reaction to cure the DERAKAN 510–A, while CoNap was used to ensure that the reaction occurred in the desired cure time. For this research, the desired cure time was 60 minutes, which provided enough time for the DERAKANE to completely penetrate all layers of the woven materials.

The above two hardeners work well if the ambient temperature is between 70˚F and 80˚F, in which case the combination of hardeners was 1.25 weight percent MEKP and 0.20 weight percent CoNap. For most of the research, the ambient temperature was well below 70˚F and a third chemical, N-dimthylaniline (DMA), was needed to ensure a cure time of 60 minutes. When DMA was used in combination with the previously stated weight percentages for CoNap and MEKP, a total of 0.05 weight percent of DMA was required. If DMA was not included at these low temperatures, cure times were much longer than the desired 60 minutes.

C. VACUUM-ASSISTED RESIN TRANSFER MOLDING TECHNIQUE

One technique for making composite materials in industry is Vacuum-Assisted Resin Transfer Molding (VARTM), which was used in this thesis to construct the three different sample sets required for testing. The VARTM process uses a vacuum to pull resin through the many layers of fiber to ensure a uniform distribution of resin throughout

the sample. This technique was extremely beneficial when working with CNTs, as they did not shift or move when the resin was run through the sample.

To begin making the two-step cured samples, a layer of peel ply was placed on a piece of glass to allow for easy removal of the sample upon completion of the VARTM process. The glass used must be at least 1.27 cm (0.5 in) thick, in order to be able to withstand the extreme heat generated during the resin curing process. When making a co-cured sample, a layer of distribution media is laid down first, covered by a layer of peel ply, as shown in Figures 4 and 5.

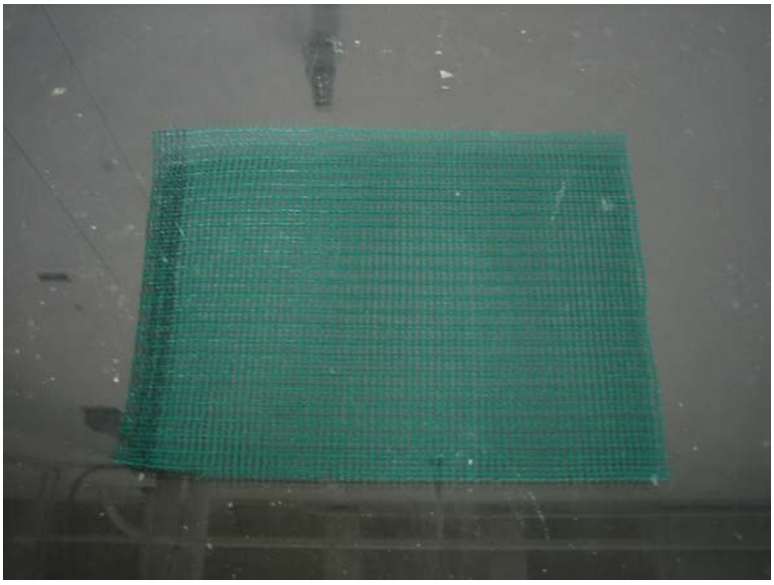

Figure 4. Bottom Layer of Distribution Media used for Co-Cured Samples

Figure 5. Peel Ply Laid on Top of Distribution Media for Co-Cured Samples

Next, the sample size was chosen and the fiber materials were cut to the appropriate size. For all samples, 10 layers of fabric were cut, five for the bottom layer, and five for the top layer. The bottom five layers were then placed on top of the peel ply, as shown in Figure 6. For the co-cure process, a Teflon film of thickness 0.0051 cm (0.002 in) was placed partially on top of the bottom five layers in order to build a crack into the sample. The last five layers of fiber material were evenly stacked on top of the fiber material and Teflon already in place. Then another layer of peel ply, followed by a piece of distribution media, was stacked on top of the complete co-cure sample. For the double-cure sample, the bottom five layers were covered with the peel ply and distribution media, as shown in Figure 7.

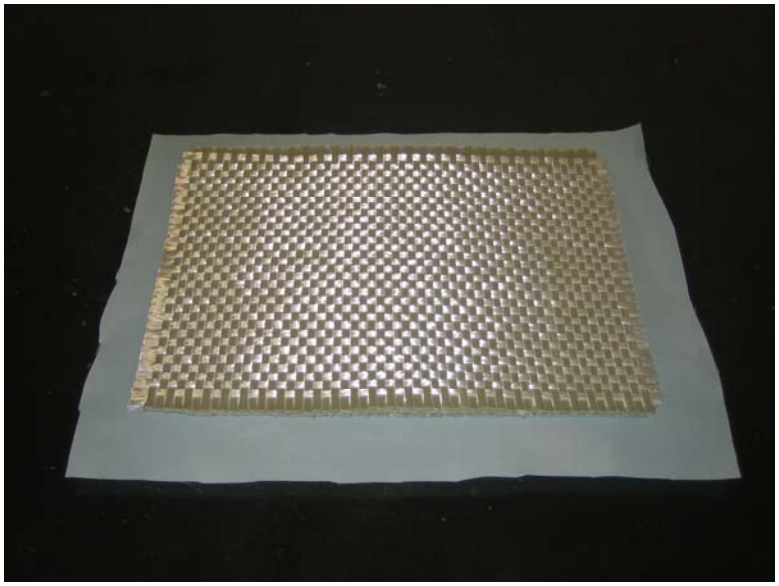

Figure 6. Bottom Five Layers of a Sample

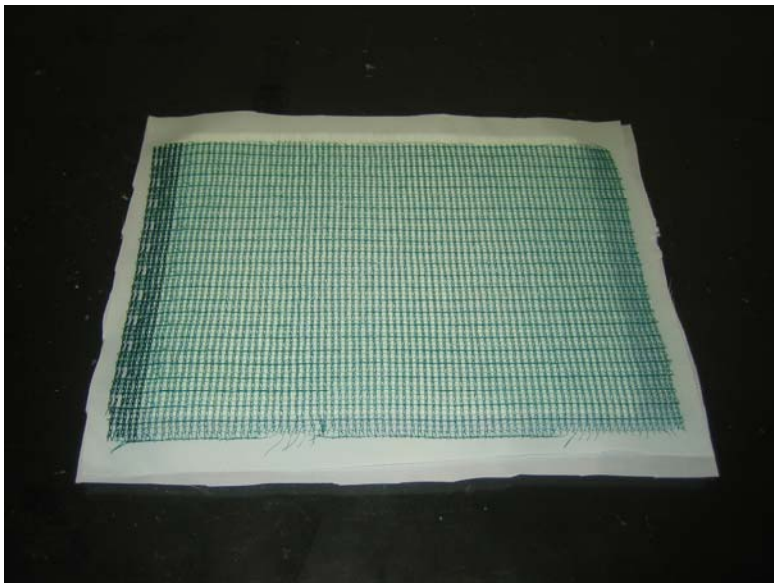

Figure 7. Peel Ply and Distribution Media on Top of Stacked Fiber Layers

In order for the resin to be pulled through the fiber material, a Rietschel Thomas Vacuum Pump model 2688CE44 was used. Tubing was hooked up to this pump and run through a gauge board to a resin trap, as shown in Figure 8. The resin trap was used to protect both the pump and gauge board from excess resin. From the resin trap, solid ½-inch diameter plastic tubing was measured and cut to be used inside the vacuum bag as the outlet for the resin. This same tubing was used to suck resin from the bottom of the

sample to the top. Attached to both the inlet and outlet tubes, and spread across the top and bottom of the sample, was spiral tubing, as shown in Figure 9. This tubing allowed for an even distribution of the resin throughout the sample.

Figure 8. Gage Board and Resin Trap

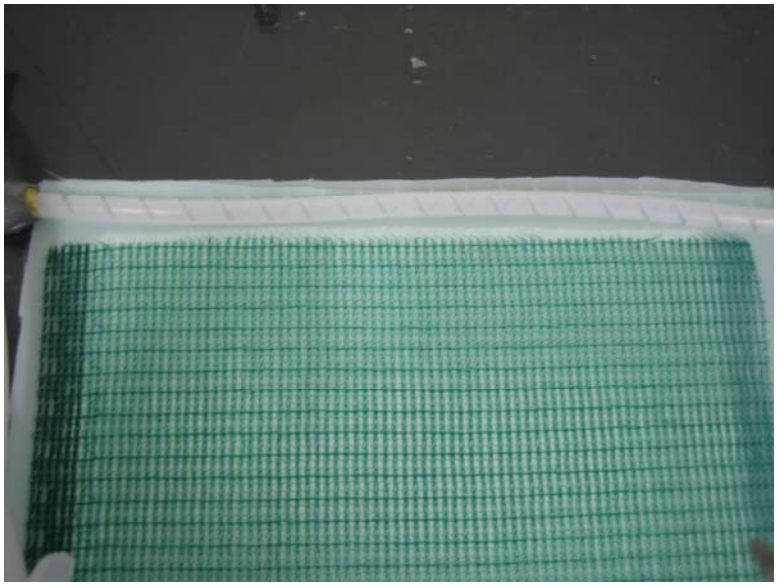

Figure 9. Spiral Tubing Used at the Top and Bottom of Sample Set-up

Once the tubing was assembled and secured, strips of vacuum bag tape were laid out in a box shape around the sample stack. The strips were placed about 2 to 3 inches

from the sample stack, so as not to interfere with the resin being run through the sample. The tape was used to hold the plastic sheet in place, which ultimately acted as a vacuum bag, Figures 10 and 11. The plastic sheet was cut to fit the square box already made, and was carefully rolled out onto the tape, Figures 11 and 12. The vacuum was turned on, and the newly-created bag was thoroughly checked to make sure there were no leaks. If there were to have been a leak in the bag, air bubbles would have entered both the bag and the sample, making the sample unusable. Once it had been verified there were no leaks, the vacuum was left on to ensure a continuous vacuum pressure throughout the rest of the VARTM process.

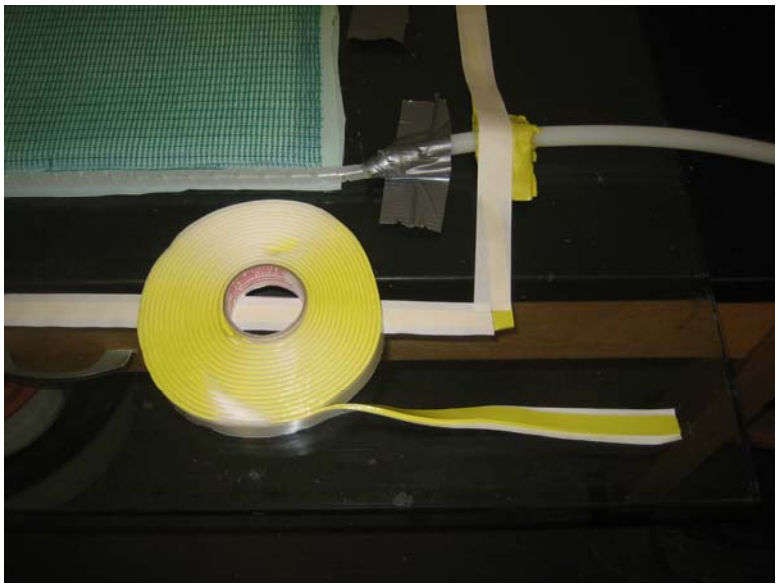

Figure 10. Vacuum Tape Used to Seal the Sample Setup

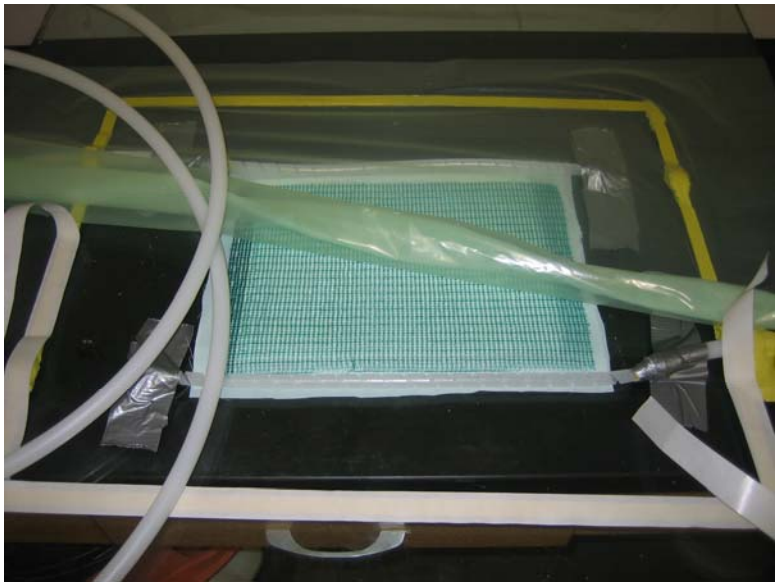

Figure 11. Rolling Out the Plastic Sheet Used to Form the Vacuum Bag

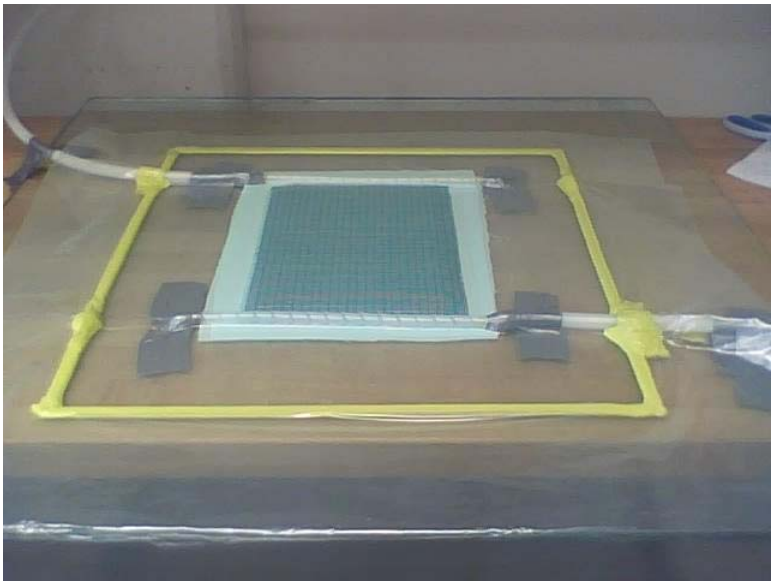

Figure 12. Sample Setup under Vacuum

While the vacuum was still running, the temperature was noted and the appropriate amounts of resin and hardeners were mixed to ensure a 60-minute cure time. Once mixed, the resin was transferred to the inlet of the vacuum bag and the inlet tube was clamped to prevent the resin from flowing through the sample. As a result of mixing and transferring the resin to a new bucket, small bubbles are formed throughout the resin, Figure 13. Enough time, about ten to fifteen minutes, was allowed for these bubbles to

dissipate before running the resin through the sample. Again, these small bubbles, if allowed to run through the sample, would have gotten caught and ruined the sample.

Figure 13. Resin at Inlet with Bubbles after Mixing

After sufficient time had passed and no small bubbles could be seen in the resin, the inlet tube was unclamped slowly to allow the resin to enter the vacuum bag. The resin flowed evenly through the sample at a steady pace, as shown in Figure 14. The resin was allowed to run all the way through the spiral tubing on the top, in order to ensure all fibers were coated with the resin as in Figure 15. One aid used to ensure that all fibers were covered with resin was the placement of the distribution media at the beginning of the VARTM setup. When both a top and bottom layers were used the bottom distribution media hung out the bottom of the sample by about ½ inch. The top distribution media was then place under the top spiral tubing and even with the bottom of the sample. This placement aided in sucking the resin up from the bottom of the sample, through the middle, and out the top.

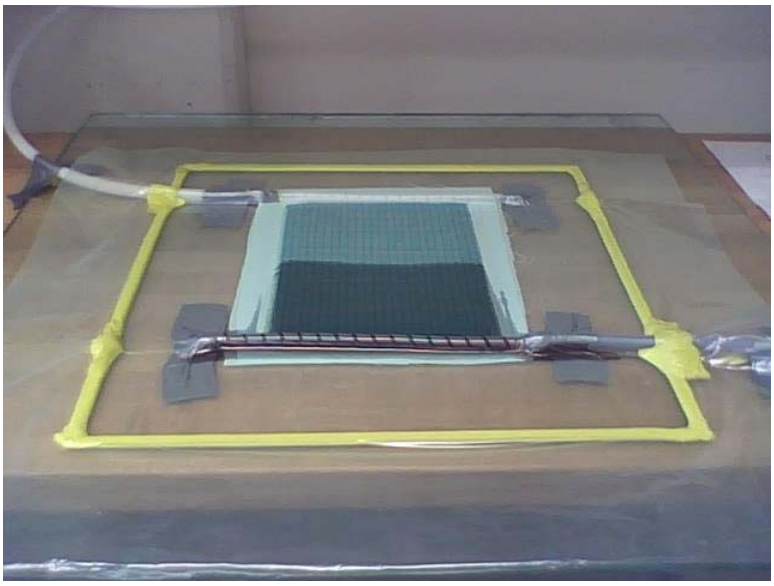

Figure 14. Resin Running through a Sample Evenly

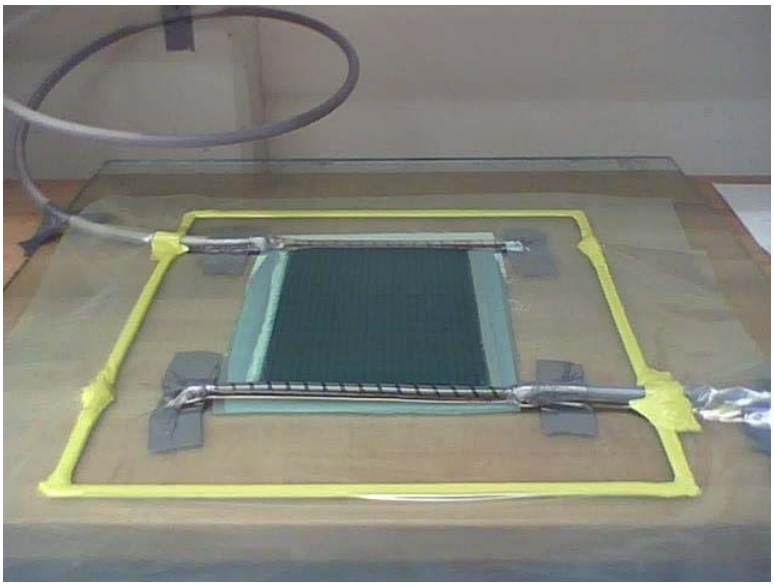

Figure 15. Resin Completely through a Sample

As the resin started to cure, it became extremely hot and started to gel. When this occurred, and all the layers were covered with resin, the resin inlet tubing was again clamped to ensure no air was pulled into the sample. The time it took for this to happen depended on the thickness and size of the sample, as well as the amount of resin and hardeners used. The sample was left with the vacuum pump running until the sample cured. If the resin and hardeners were mixed and added correctly, this was about 60

minutes. After this time, the pump was shut off, but the sample was left at least 12 hours to ensure complete curing of the sample. At this point, the co-cured sample was complete and was taken to a water jet to get cut into the correct coupon size. For the two-step cured process more work was needed to complete the sample.

Since the bottom layer of the two-step cured sample was the only thing made the first time through, the initial crack and top layer were then manufactured. To do this, the first start step was to take the newly-made bottom layer, and sand the top surface with 100 grit sand paper in order to roughen the surface. Next, the sanded surface was cleaned with acetone, in order to make sure that all sanded particles are removed. The acetone was allowed to fully dry before continuing the VARTM process. When working with CNTs, they were dispersed over the top of the entire sanded composite plate using acetone, and again ensuring enough time was allowed for the acetone to dry, as shown in Figure 16.

Figure 16. Bottom Layer of Double-Cure Sample Covered With CNTs

For sample sets two and three, thin pieces of stainless steel plates were fastened to the top and bottom of the sample, as shown above in Figure 16. The stainless steel was needed to allow for a place to secure conductive test equipment to the sample and not interfere with any other testing. For all other samples, this step was skipped.

Finally, the same steps as before were followed. Peel ply was laid on the glass followed by the bottom composite plate. The crack was formed using the same Teflon material as before and is shown in Figure 17. The previously-cut five pieces of fiber material used to make the top plate were carefully stacked on top, Figure 18. More peel ply was used, again followed by a piece of distribution media on top. Tubing was cut, tape was laid out, and the vacuum bag was sealed and tested. The resin was then mixed, allowed to sit while bubbles were popped, and then the resin was run through the sample. The resin got hot, gelled, and 60 minutes later it was completely cured and the pump was shut off. Again, the sample was given about 12 hours to sit and fully set. The two-step cured sample was complete and was taken to be cut using a water jet.

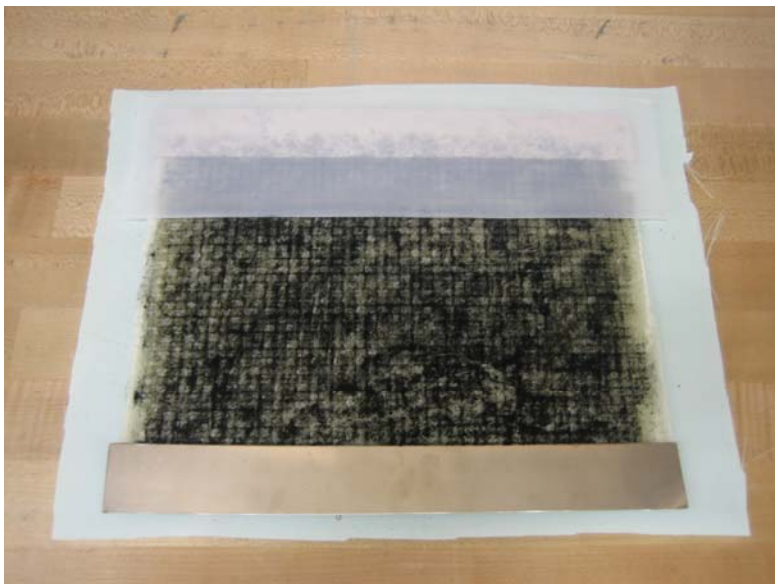

Figure 17. Teflon Layer Used to Build Initial Crack in Sample

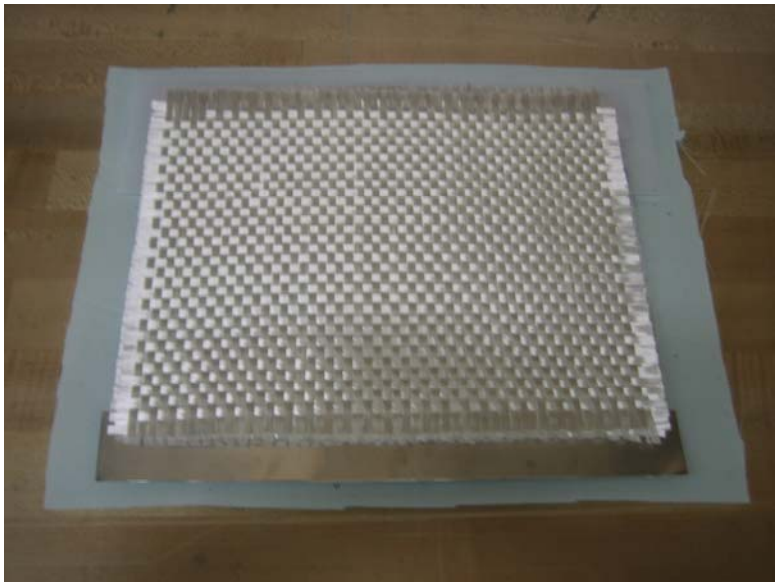

Figure 18. Remaining Fiber Material Stacked on Top of Bottom Plate

THIS PAGE INTENTIONALLY LEFT BLANK

III. PHASES OF RESEARCH

A. PHASE I: FAMILIARIZATION

Phase I consisted of a familiarization stage, during which samples were constructed to simply learn the finer ins and outs of the VARTM technique. Several samples were constructed, but only the last few were usable. The samples that did not turn out were cut open and examined to help correct the problems. The good samples were cut into coupons and tested in order to learn how to use the test equipment, but no data was collected.

B. PHASE II: CO-CURED VS. TWO-STEP CURED

Phase II was conducted in order to determine the validity of using a co-cure method versus a two-step cure method when making samples. This phase consisted of two different sets of carbon composite samples that did not include CNTs. Samples were cut into coupons 2.4 cm wide, 0.42 cm thick, and 17 cm long, based on applicable ASTM Standards. The coupons were tested in Mode II and critical strain energy release rate, G, was calculated.

C. PHASE III: CARBON COMPOSITE RESISTANCE TESTING

Once Phase II was complete, two new carbon composite sample sets were constructed. One set of samples was the same as the Phase II two-step cured samples, while the other sample set included a layer of CNTs dispersed through the center of the sample. CNTs surface concentration was 7.5 g/m^2 and was dispersed using acetone. The selection of CNTs surface concentration, as well as the selection of acetone as the dispersing agent, was based on results from compression testing of CNTs reinforced scarf joints conducted during previous research.[17] Additionally, built into each sample set at the far ends were thin pieces of stainless steel metal. This was used in order to prevent a

[17]Y. W. Kwon, R. Slaff, S. Bartlett, and T. Greene, "Enhancement of Composite Scarf Joint Interface Strength through Carbon Nanotube Reinforcement," *Journal of Materials Science* (2008): 1–9.

larger crack in the sample than was used in Phase II, but to allow for electrical testing to be conducted. These sample sets were cut into the same size coupons as used in Phase II.

The purpose of this phase of research was to determine if a layer of CNTs could be used to detect crack propagation making use of the CNTs' electrical conductive nature. Both sets of samples were tested in Mode II, while an electrical current was run through them and the resistance was monitored. The resistance changes before, during, and after Mode II testing were noted and critical strain energy release rate, G, was calculated.

D. PHASE IV: FIBERGLASS COMPOSITE RESISTANCE TESTING

Upon completion of Phase III, the exact same size sample sets used in Phase III were constructed and cut into the same coupon sizes, except fiberglass was used as the base composite material. To ensure the CNTs were allowed to touch one another, a CNTs dispersion concentration of 10 g/m^2 was used. The purpose of the phase was to determine if the CNTs' electrical conductivity could be exploited in even lesser conductive composite materials. Ideally, even in low conductive materials, some current will flow through the CNTs middle layer, allowing for crack propagation to be detected. Both sets of samples were tested in Mode II, while an electrical current was run through them and the resistance was monitored. The resistance changes before, during, and after Mode II testing were noted and critical strain energy release rate, G, was calculated.

E. PHASE V: RESIS TANCE RE LIABILITY AND CRACK GROWTH RELATIONSHIP TESTING

This phase put both the carbon and fiberglass composites reinforced with CNT in Phases III and IV through more tests. These tests were designed to determine the reliability of the resistance readings collected in Phases III and IV, as well determine if there is a relationship between the changes in crack length to the changes in resistance.

The first test used the previously cracked sample sets with CNTs from both Phases III and IV, and slowly loaded them to a desired load prior to the point of further

crack propagation. The resistance readings were then read while under load, and then upon unloading of the sample. This step was then repeated several times to determine the consistency of the resistance readings.

For the second test, the crack length acquired during previous phases of research, for each coupon, was measured along with the corresponding resistance reading. The cracked coupon was then placed under a high enough load for the crack to propagate. Upon propagation of the crack, and while still under load, a resistance reading was taken. The load was removed and another resistance reading was measured. This procedure was repeated until it was no longer possible to propagate the crack further. The resulting data was used to determine relationships between change in crack length and change in resistance readings.

THIS PAGE INTENTIONALLY LEFT BLANK

IV. TES TING

A. EQUIPME NT

All tests were conducted using an Instron Tension/Compression Machine (Model Number: 4507/4500), shown in Figure 19. All testing phases were conducted using a 10 kN load cell. Collection of data generated by the Instron Machine was done by a Series IX computer software which was also used to control the Instron to achieve desired test requirements. Additionally, for Phase III, IV and V the coupons were hooked up to a Fluke 8840A Multi-meter as displayed in Figure 20. This device was used to measure the resistance within the coupons throughout the entire test period. Data produced from this machine was collected by hand at 30-second intervals.

Figure 19. INSTRON Mode II Test Setup

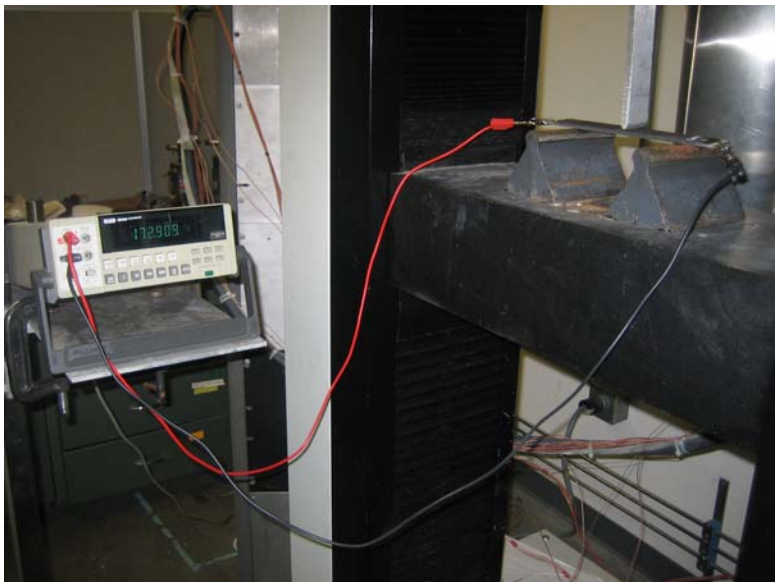

Figure 20. Fluke 8840A Multi-Meter and INSTRON Mode II Test Setup

B. PROCEDURE

In order to model a Mode II fracture, in which only shear force affects crack propagation, each sample set was tested using a three-point bending test. This test was chosen based on previous research conducted.

The setup used is shown in Figures 21 and 22. For all tests, the Instron held the center support stationary, attached to the load cell, while the base supports were incrementally moved up into the stationary support. The higher the base moved the greater the load felt on the coupon became, resulting in higher shear stresses felt at the crack tip. A plot of force versus displacement was provided from the Series IX computer software and used to help calculate the Mode II critical strain energy release rate, $G_{II.}$

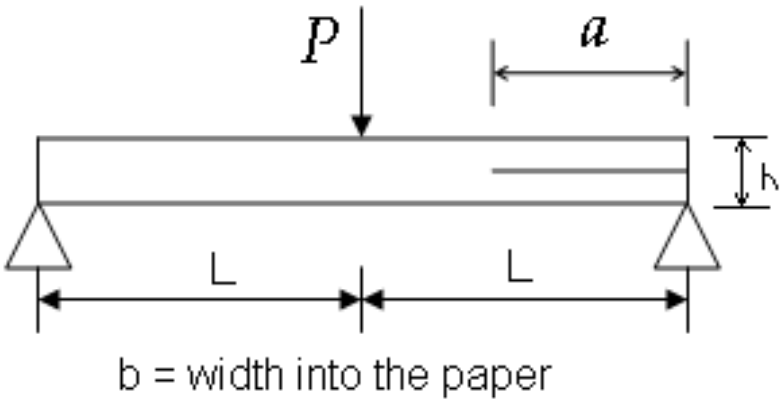

Figure 21. Diagram of Three-point Bending Test for Mode II[18]

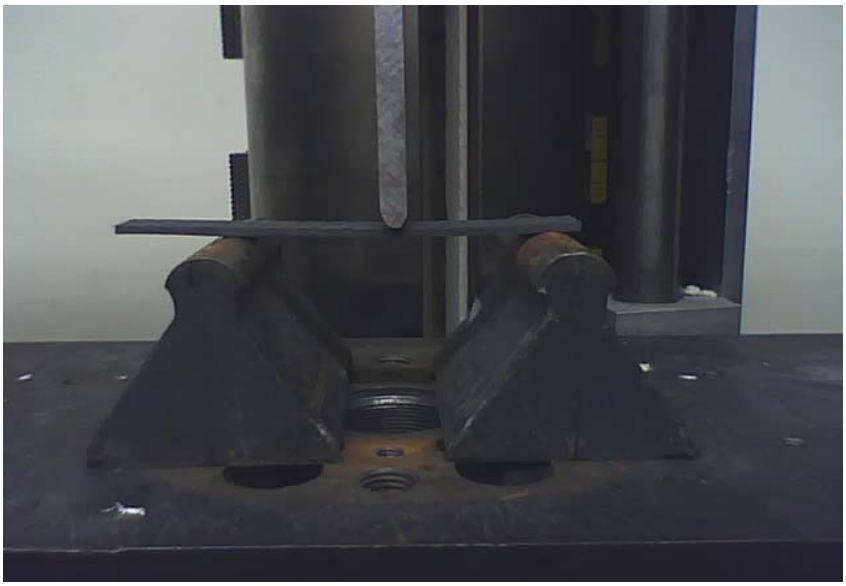

Figure 22. Picture of Three-point Bending Test for Mode II

Additionally, during Phase III, IV and V testing, the resistance of each coupon was monitored. At the point of crack propagation, the resistance through the coupon was annotated and compared to that of the initial resistance reading. The resistance was again taken after the test had stopped and the coupon was still bent. Another reading was taken after the coupon was removed from the Instron and returned to a load free state.

[18] Faulkner, "Study of Composite Joint Strength with Carbon Nanotube Reinforcement," 19.

C. CALCULATIONS

In order to calculate the Mode II critical strain energy release rate, G_{II}, a compliance method was used, which is based on the slope of the force versus displacement load obtained during testing, i.e., a linear slope before crack propagation. Once the compliance is obtained, the following equation is used to calculate G_{II}:[19]

$$G_{II} = \frac{9a^2 P_c^2 C}{2b(2L^3 + 3a^3)}$$

The initial crack length (a), coupon width (b), and the span length (2L) are all dependent on coupon geometry pre-determined prior to the start of the test. The critical load, P_c, was determined based on the local maximum or slope change in the load versus displacement curve, as well as observation. Compliance was determined after the completion of the test by taking the inverse of the slope of the load versus displacement prior to crack propagation.

The compliance method is actually one of two ways to calculate G_{II}. The first method based on the Modified Beam Theory method requires material properties to be known, as well as precise measurement of height and thickness of the samples. The second method, the compliance approach, was chosen as it does not require material properties be known. Although it could easily be determined what these material properties are, they vary depending on the CNT included and the thickness of coupon. The compliance approach indirectly measures the material properties when calculating the compliance.

No additional calculations were required for Phase III and IV resistance testing. All data collect was already in the desired form of resistance measurements. For Phase V the slope of the line formed by data points on the crack length versus resistance reading graphs were calculated.

[19]M. Todo, T. Nakamura, and K. Takahashi, "Effects of Moisture Absorption on the Dynamic Interlaminar Fracture Toughness of Carbon/Epoxy Composites," *Journal of Composite Materials* 34(2000): 630–648.

V. RESULTS AND DISCUSSION

A. PHASE I: FAMILIRIZATION

During this phase, several samples were made although very few were useable. The first four sets of samples constructed were four times thicker than those ultimately tested in follow-on phases. The first two of these samples did not turn out properly due to a leak in the vacuum bag seal that, even after repair, allowed too much air in to salvage the sample. The third sample did not turn out to be good due to the thickness of the sample, and the inability of the pump to completely pull the resin through the entire sample. To fix this problem, on the fourth sample an extra strip of distribution media was used in the middle bottom portion of the sample. This allowed for three different paths for the resin to follow, ensuring the middle of the sample was thoroughly infused with resin. On most days this sample would have turned out correctly, but it never gelled in time allowing air to enter in. This is when it was discovered that, for most of the year in Monterey, CA, N-dimthylaniline (DMA) is required to ensure proper resin cure times.

The last two samples constructed in Phase I were used to ensure that all procedures consistently worked. With the use of DMA included in the resin and hardener mixture, all samples were made successfully. These samples were not put through Mode II testing, but were used to test new cutting techniques. Normally, samples of this nature are cut into coupons using a water jet, but after trial and error it was determined that a band saw with the correct blade can also cut composite samples.

B. PHASE II: CO-CURED VS. TWO-STEP CURED

The first coupon tested was a two-step cured coupon with a 2.6 cm initial crack length, span length of 15 cm, and width of 2.4 cm. The load was applied in the middle of the span length at a location of 4.9 cm from the crack tip. Prior to signs of crack propagation, this coupon failed at the point of the load application. This was not what was desired, and so the speed was slowed down to 0.5 mm/min from 1 mm/min. This was done in order to ensure that bending stress within the sample were not larger than failure stresses.

The second coupon, tested with the new test speed, was also a two-step cured coupon with the same geometry. Again, the coupon failed at the point of load application prior to any crack propagation. Since the crack length was relatively small compared to the span length, in both tests the load was applied too far away from the crack tip. Bending stresses were reached prior to the onset of crack propagation.

To correct for this problem, the base supports on the Instron were moved closer together to reduce the span length by one cm. The next coupon tested was two-step cured, with the same crack length and width. Again the coupon failed at the point of load application. A fourth two-step cured coupon was tested after moving the base supports in an additional one cm. This time the crack began to propagate prior to buckling failure at the point of load application. This failure corresponded to a span length of 13 cm, and placed the load application much closer to the crack edge.

The span length of 13 cm was used for two more two-step cured coupons without experiencing any more failures due to bending. However, this was not the case for all coupons, as again bending failure was experienced on another coupon. The span length of 13 cm was found to be the borderline length where either bending or crack propagation could occur. A new span length of 12 cm was found to be an ideal length, and all other coupons were tested using this span length.

The ratio of crack length to one-half the span length for the 15 cm span length was found to be 0.35. The ratio for a span length of 13 cm, which appeared to be the borderline span length, was 0.4. This shows that, for this particular sample set, a ratio of crack length to one-half the span length for the test speed of 0.5 mm/min should be greater than 0.4. For this particular sample set, such a ratio ensures that bending stresses are not exceeded prior to the stress required for crack propagation.

Once a set span length was acquired, test results showed that there was a slight increase in G_{II} for two-step cured coupons over that of co-cured coupons. Figure 23 shows the normalized average values of G_{II} for Phase II coupons, including the standard deviation among the coupons tested. This data indicates that the two-step cured sample sets had G_{II} values 3.8% higher than the co-cured sample sets. The actual values of each

coupon can be seen in Appendix A. From this it is important to note that two-step cured coupons had a wider range of G_{II} values, but most of them were higher than that of the co-cured coupons.

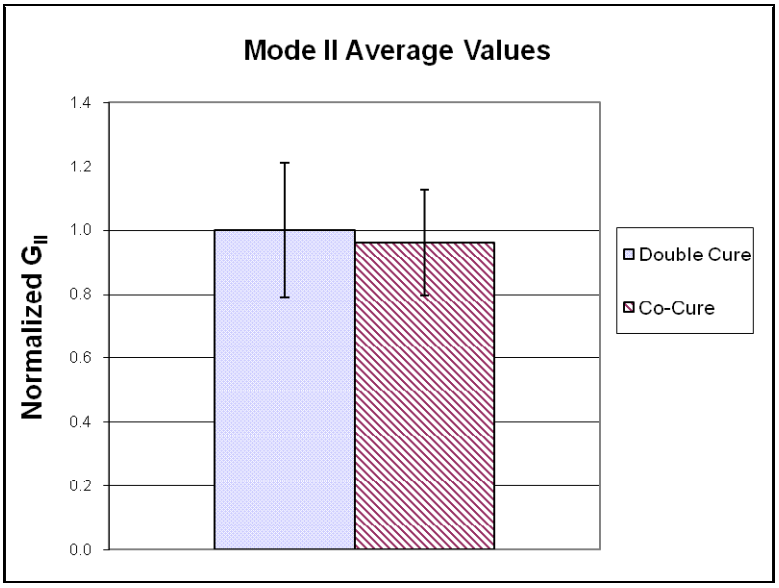

Figure 23. Normalized Average Values of G_{II} for Phase II

Upon further investigation, it was observed that the crack propagation was similar for both the two-step cured and co-cured sample sets. For both cases, the crack initially propagated from the built-in crack tip and ran along the centerline of the coupon perpendicular to the load application. Figures 24 and 25 show the path of crack propagation as described.

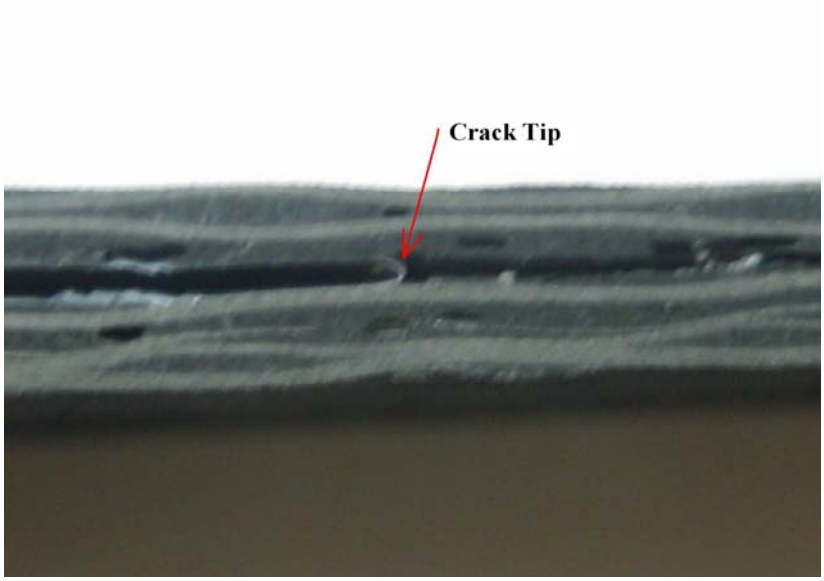

Figure 24. Crack Propagation Path for a Co-Cured Coupon

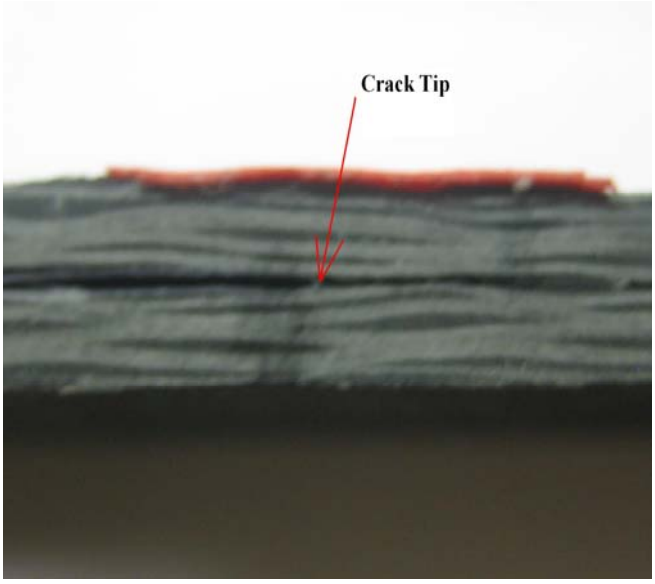

Figure 25. Crack Propagation Path for a Two-Step Cured Coupon

After testing was complete, coupons in which crack propagation occurred were pulled apart to inspect the cracked surface. Both the co-cured and two-step cured

coupons experienced the same type of failure. In some areas, the joint interface bond was broken through the resin, while in others the resin was pulled away from the fibers, as shown in Figures 26 and 27.

Figure 26. Surface Crack Propagation Path for a Co-Cured Coupon

Figure 27. Surface Crack Propagation Path for a Two-Step Cured Coupon

Since both the co-cured and two-step cured samples failed in a similar manner, a probable cause for the two-step cured higher G_{II} values is related to the VARTM process.

When making two-step cured samples, the surface of the bottom resin layer is sanded and cleaned carefully with acetone. During this process micro-scale defects, like voids in the resin layer, are reduced, allowing for a stronger boundary interface to form between the top and bottom fiber layers.

C. PHASE III: CARBON COMPOSITE RESITANCE TESTING

This phase began with Mode II testing of all carbon composite coupons containing CNTs. Based on Phase II results, a ratio of crack length to one-half the span length of greater than 0.4 was desired; as a result, the initial crack length was chosen to be 4 cm, with a span length of 16 cm, and width of 2.4 cm. These geometry parameters resulted in a ratio of 0.5, which with a Mode II test speed of 1 mm/min, resulted in coupon failure through crack propagation.

Prior to the start of testing each coupon was measured to determine its resistivity for baseline comparisons. Each of these starting resistance readings can be seen in Appendix B, and shows a varying degree of starting resistances. This is due to the unevenly spread CNT, directly resulting from the dispersion technique used during the VARTM process. Each value recorded however, was constant to within a tenth of an ohm, and was read several different times before recording values.

During the actual testing, values of the resistance readings were recorded manually at 30 second intervals. These values varied little from the initial readings throughout the entire test. In fact most of the averages of these readings, with the exception of those coupons with higher initial resistance readings, matched within 14% of the initial resistance readings. Even when the sample cracked and continued to crack, the resistance readings stayed constant varying only a few ohms at a time. The averages resistance readings throughout the test are summarized in Appendix B.

When the test was complete the sample was left in the bent position shown in Figure 28. The readings taken in the bent position were again constant, only fluctuating to the tenth of an ohm, and within 4% of the initial resistance values. When the coupons were released from this bent position, the resistance readings for all coupons increased, and are listed in Appendix B. Again the variance in the increase percentage can be

contributed to the CNT dispersion method used during the VARTM process. On average the increase in resistance readings for carbon composite coupons with a layer of CNTs was 15.7%. This increase in resistance is what is desired in order to use CNTs as a possible NDT method.

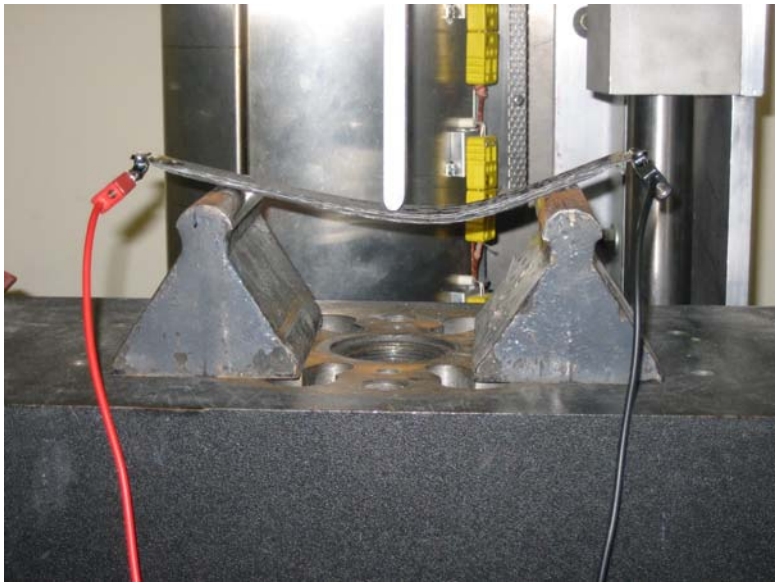

Figure 28. Carbon Fiber Mode II Resistance Testing Bent Position

After experiencing such positive results from the carbon composite CNTs reinforced coupons, the pure carbon composite coupons were tested. The first coupon tested was setup with the same geometric parameters and Mode II test speed. However, since the speed was faster than that used in Phase II, the coupon failed through bending in the middle at the point of load application. Another pure carbon composite coupon was tested to ensure that these test parameters were faulty for pure carbon composite coupons. This second coupon failed in the same manner, and as a result the geometric parameters were changed for the rest of the coupons. The remaining eight coupons were tested having an initial crack length of 4 cm, a span length of 15 cm, and width of 2.4 cm.

Again prior to the start of testing, each coupon was measured to determine its resistivity for baseline comparisons. Each of these starting resistance readings can be seen in Appendix C, and shows a varying degree of starting resistances. For the pure carbon composite coupons the resistance readings were very inaccurate and by no means

repeatable. Each time the coupons were hooked up to the multi-meter they started at a given value and fluctuated widely. After fluctuating for a little bit, all coupons' resistance readings began to steadily increase, acting as a capacitor. This was an unexpected result, but validated the conductive behavior of CNTs when included in carbon composites.

For pure composite coupons the resin, which is non-conductive in nature, is what is being measured for resistance. Unfortunately, instead of acting as an open circuit, as would be expected of a non-conductive material, the resin layer behaved as a capacitor. Since the thickness of the layer of resin, compared to that of the surrounding carbon, was thin, the carbon was able to sense some of the electricity being run through the stainless steel. This flow of electricity was then transferred to the resin. The resin was charged by the surrounding carbon, and in essence became a capacitor.

During Mode II testing of the pure carbon composite samples, resistance readings were recorded manually at 30 second intervals. These values typically started high and as the load was increased, they gradually decreased. For each coupon tested, at a certain point during the Mode II testing, the values became steady and unchanging. These values were extremely low in comparison to the initial fluctuating values experienced prior to testing. The low steady resistance readings were a result of the sample being placed under stress. When placed under stress, the carbon was not able to charge the resin layer as it had before. Instead, the resin layer was compressed and too small for the carbon to charge. The low readings, were in fact, those of the carbon layers.

When the test was complete, the coupon was left in the bent position and a resistance reading was recorded. Readings taken in the bent position, for all pure carbon composite coupons, were steady only fluctuating to the tenth of an ohm. These resistance readings were extremely low compared to the initial readings taken, and are given in Appendix C. Also given in this appendix are the average resistance values felt during Mode II testing.

When the coupons were released, and returned to a flat position, an additional resistance reading was taken. The resistance, for all pure carbon composite coupons,

increased, and then steadily began to climb, again taking on the behavior of a capacitor. The values recorded in Appendix C are the values taken upon initially being returned to the flat position. All readings are the baseline from which the resistance started to quickly grow. Thus, unlike the carbon composite coupons with CNTs, the pure carbon composite coupons respond poorly to the electrical resistance test. NDT could not be used for pure carbon composite coupons, but is a valuable technique for carbon composite reinforced with CNT.

To ensure that this was still a valuable use for the strengthening of composites at areas of high concentration, and verify the results of previous research done at NPS, the G_{II} values for both the carbon composites with and without CNTs were calculated. Figures 29 and 30 show each coupon's load versus extension graphs used to calculate the required G_{II} values. The two graphs show that carbon composites hold load the same way for both with and without CNTs, however, the crack location for composites with CNTs is prolonged. Those coupons with CNTs also were able to reach higher loads before complete load failure. This was verified by the test results that showed there was an increase in G_{II} for carbon composite coupons with CNTs over that of pure carbon composite coupons. Figure 31 displays the normalized average values of G_{II} for Phase III coupons, along with the respective standard deviations. This data indicates that the carbon composite sample sets reinforced with CNTs had G_{II} values 20% higher than the pure carbon composite sample sets. The actual values of each coupon can be seen in Appendix D. From this it is important to note that each sample set had a similar standard deviation, and that the highest value of the pure carbon sample set was barely higher than the lowest sample set coupon reinforced with CNT.

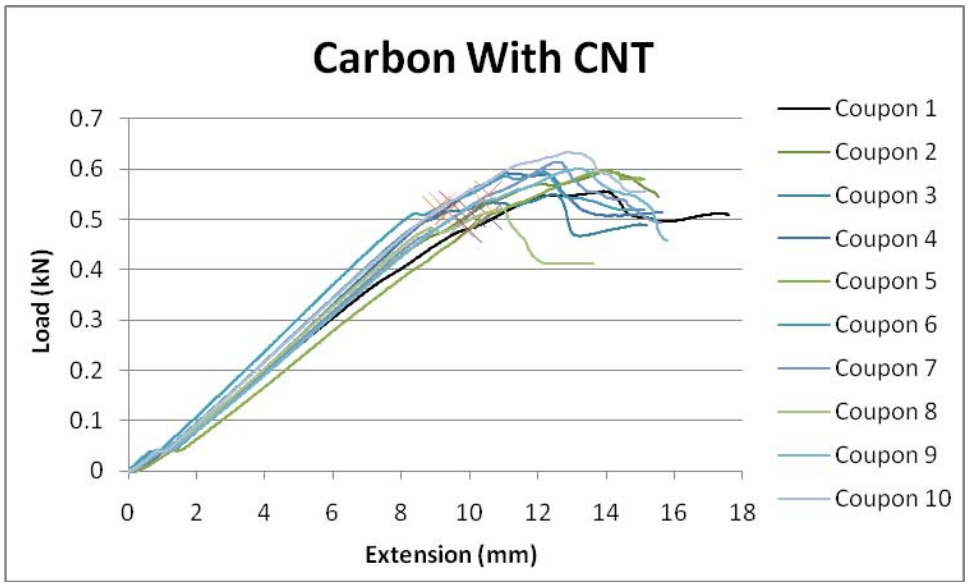

Figure 29. Mode II Graph of Carbon Composites With CNT

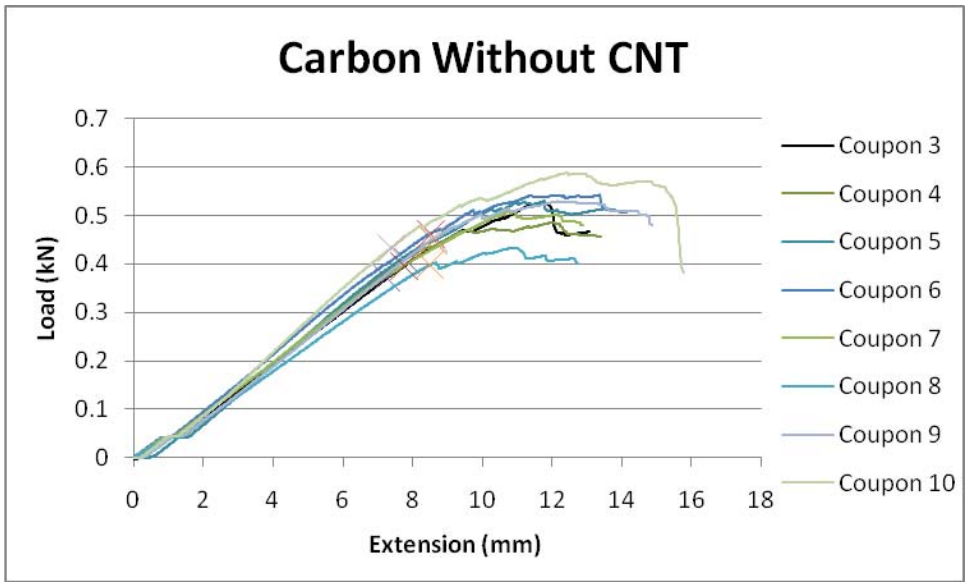

Figure 30. Mode II Graph of Carbon Composites Without CNT

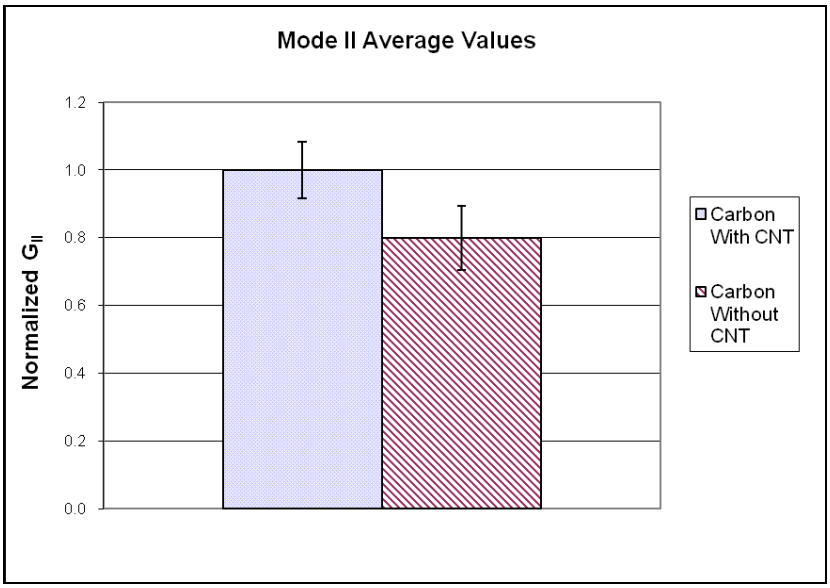

Figure 31. Normalized Average Values of G_{II} for Phase III

Based on previous research conducted at NPS[20], the layer of CNTs included within the carbon composite acted as expected. The pure carbon composite samples experienced crack propagation at the initial crack tip, followed by propagation through the joint interface. Carbon composites with CNTs, first experienced cracking at areas away from the crack tip, i.e., weaker zones. These cracks then propagated back towards the initial crack tip. These different crack propagations can be verified by observing the surface of the joint interfaces where cracking occurred. Figure 32 shows the relatively smooth joint interface of a pure carbon sample, with little fibers broken. This is a result of the crack propagating through the joint interface. Figure 33 on the other hand shows the rougher joint interface of the carbon composite containing CNTs. The rough surface has CNTs on both sides, as well as several areas were the crack propagated back to the initial tip through fibers. The crack was forced to propagate through the fibers due to the CNTs being located in the joint interface strengthening it and making it resistance to crack propagations.

[20] Faulkner, "Study of Composite Joint Strength with Carbon Nanotube Reinforcement," 27–30.

Figure 32. Surface Crack Propagation Path of Carbon Composite Without CNT

Figure 33. Surface Crack Propagation Path of Carbon Composite With CNT

D. PHASE IV: FIBERGLASS COMPOSITE RESISTANCE TESTING

This phase began with Mode II testing of all fiberglass composite coupons containing CNTs. Based on the results of Phase II, the initial crack length was chosen to be 4 cm, with a span length of 16 cm, and width of 2.4 cm. These geometry parameters along with a Mode II test speed of 1 mm/min, resulted in coupon failure through crack propagation.

Prior to the start of testing each coupon was measured to determine its resistivity for baseline comparisons. Unfortunately, only four of the coupons made actually registered any resistance on the multi-meter. An advantage to using fiberglass for testing is that the CNTs inside the fiberglass composite could easily be seen. For the six coupons that did not conduct, large areas within the coupons that were devoid of CNTs could be detected as shown in Figure 34. Each of the four coupons that did conduct had a visual path of CNTs that were continuous throughout the entire length of the coupon, as displayed in Figure 35. This shows that in order for CNTs to be effective, they must be touching. At the same time though, it also shows that if the CNTs are touching, they can be effective even in non-conductive base composite materials. In order to ensure that CNTs are touching, a better method for dispersion during the VARTM process should be developed. A better method of dispersion would result in no open gaps, as experienced in this particular sample set. All of the samples had large areas on one side or the other were CNTs could not be seen. Figure 32 and 33 both shown areas on the top which are a result of the Teflon used to create the cracks, however, the one in the middle on the bottom are in fact devoid of CNTs. Again this is a result of the VARTM process and the uneven dispersion method used.

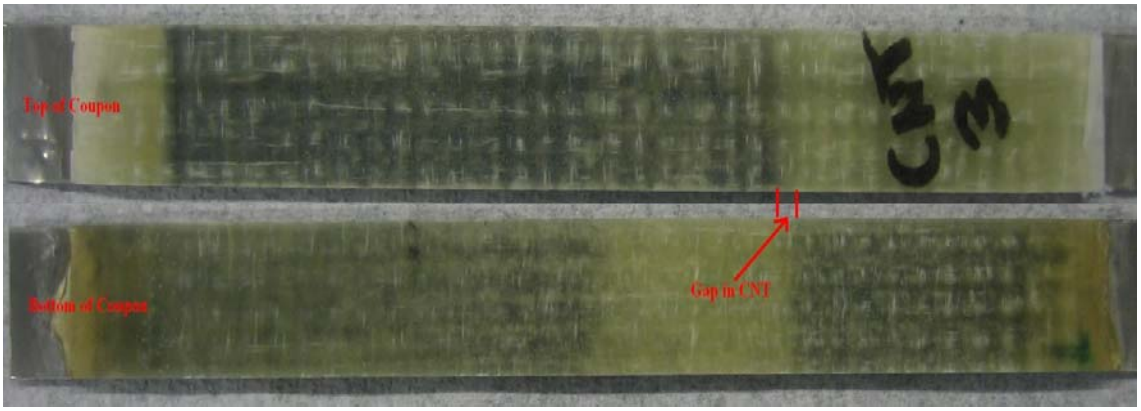

Figure 34. Fiberglass Coupon With Gaps in the Layer of CNTs

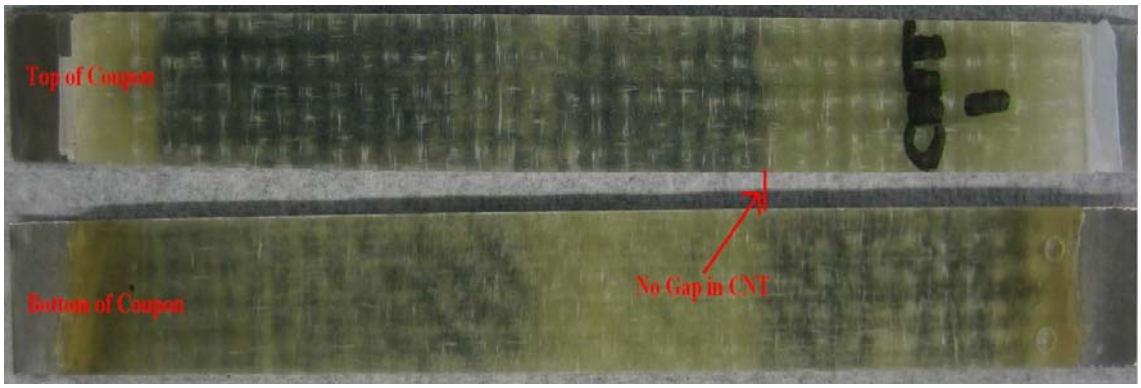

Figure 35. Fiberglass Coupon With Continuous Layer of CNTs

Even though only four of the coupons were conductive, all coupons containing CNTs were put through Mode II testing and values of the resistance readings were recorded manually at 30 second intervals. The six coupons that initially did not conduct, still registered no readings during the entire test. The values for the four conducting fiberglass coupons, although much higher than those obtained for the carbon composite coupons in Phase III, showed the same steady trend. During the test the resistance readings varied little from the initial readings, and matched within 6%. Even when the sample cracked and continued to crack, the resistance readings stayed constant varying only a few ohms at a time, again consistent with Phase III carbon composite coupons with CNTs. The average resistance readings throughout the test are summarized in Appendix E.

When the test was complete the sample was left in the bent position as was done during Phase III. The six coupons that were non-conductive still registered no resistance; however the remaining four continued to give constant resistance readings. The readings in the bent position were constant, but all readings had increased from the initial values, some by as much as 30%. When the coupons were released from this bent position, the four conducting fiberglass coupon's resistance readings continued to increase while the non-conduction fiberglass coupon's remained unchanged. Both the bent and flat readings for the four conducting fiberglass coupons are listed in Appendix E. Although each coupon showed an increase in resistance, some showed higher percentages than others. This variance can be contributed to the CNT dispersion method used during the VARTM process. On average the increase in resistance readings for fiberglass coupons with CNTs was 42.9%. Although much higher, this increase was consisted with Phase III results, and is even more significant since it occurred in a non-conductive base material.

Next, the pure fiberglass coupons were tested. For these coupons resistance readings were simple to take throughout the entire testing process. Each of the ten coupons manufactured were tested and each one acted as an open circuit before, during and after Mode II testing. This was what was expected of a non-conducting base composite material, and is exactly how the fiberglass composite samples with gaps in the CNTs behaved. This is evidence that proofs further, that in order for CNTs to be effective, they must be touching. When touching, CNTs will conduct and can be sensed by a simple multi-meter.

Research, previously conducted with CNTs at the Naval Postgraduate School, focused on the use of CNTs to strengthen carbon composite structures.[21] Therefore it was important to know if CNTs would strengthen fiberglass composites in the same way that they do carbon composite structures. To do this, the G_{II} values for both the fiberglass composites with and without CNTs were calculated. Test results showed that there was an increase in G_{II} for fiberglass composite coupons with CNTs over that of pure fiberglass coupons. Figure 36 displays the normalized average values of G_{II} for Phase IV

[21] Faulkner, "Study of Composite Joint Strength with Carbon Nanotube Reinforcement,"1–42.

coupons, along with the respective standard deviations. This data indicates that the fiberglass composite sample sets with CNTs had G_{II} values 35% higher than the pure carbon composite sample sets. The actual values of each coupon can be seen in Appendix F. From this it is important to note that the highest value of the pure fiberglass sample set was barely higher than the lowest sample set value for fiberglass with CNTs.

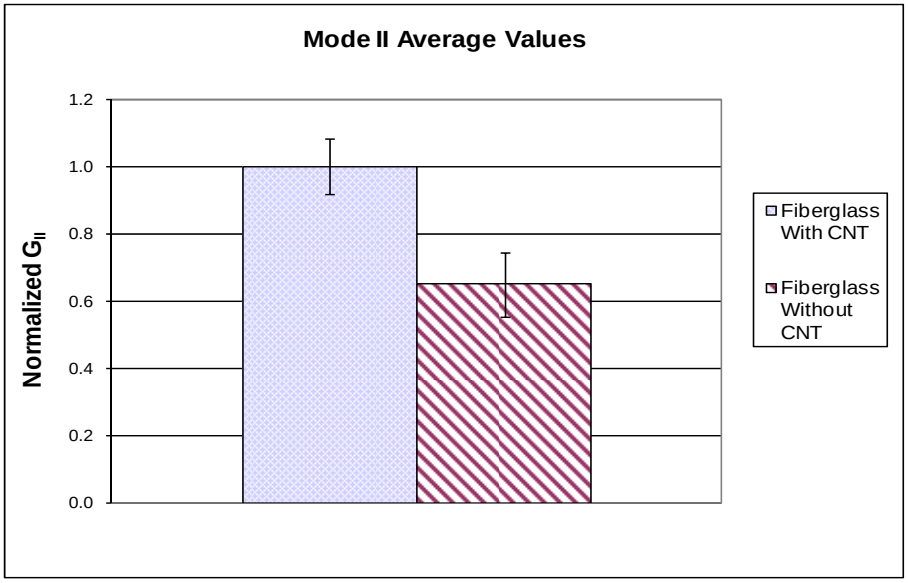

Figure 36. Normalized Average Values of G_{II} for Phase IV

When testing the carbon composites in Phase III, for both with and without CNTs, the way in which they failed was expected based on previous research already conducted.[22] Fiberglass however, was surprising in its behavior both with and without CNTs. During testing of fiberglass coupons with CNTs, a loud cracking sound could be heard upon failure followed by a quick decrease in the loading. This can be seen in Figure 37, which displays the load versus extension graph for all fiberglass coupons with CNTs. The peak of each graph closely corresponds to the crack propagation point observed visually, audibly, and graphically. This loud cracking sound was not observed during testing of fiberglass composites without CNT, instead a soft crackling sound could be heard. Also with the pure fiberglass coupons, after the crack could be visually and

[22] Faulkner, "Study of Composite Joint Strength with Carbon Nanotube Reinforcement," 22–31.

audibly verified, loads being applied still continued to climb. This can be shown in Figure 38, which also displays the location where the crack could be seen and heard.

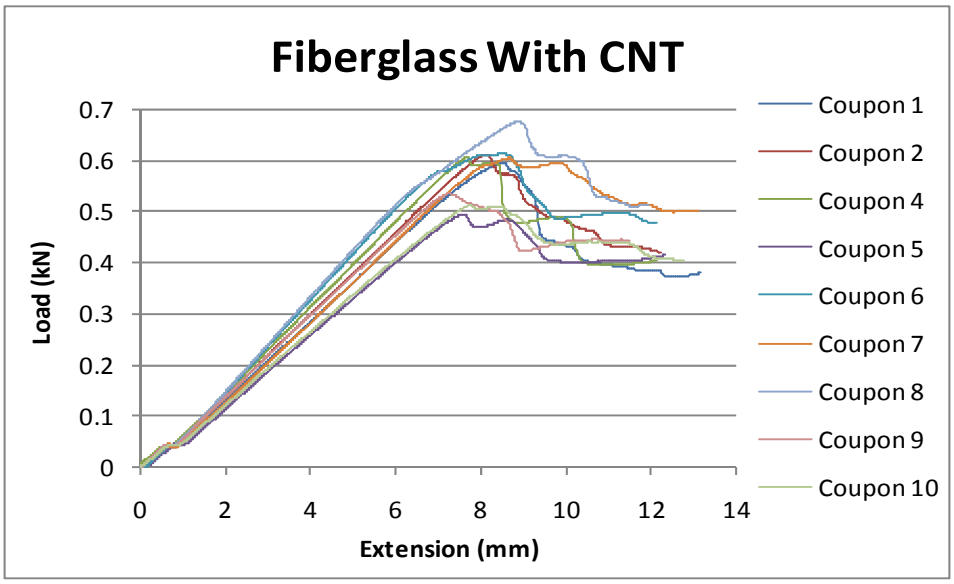

Figure 37. Mode II Graph of Fiberglass Composites With CNT

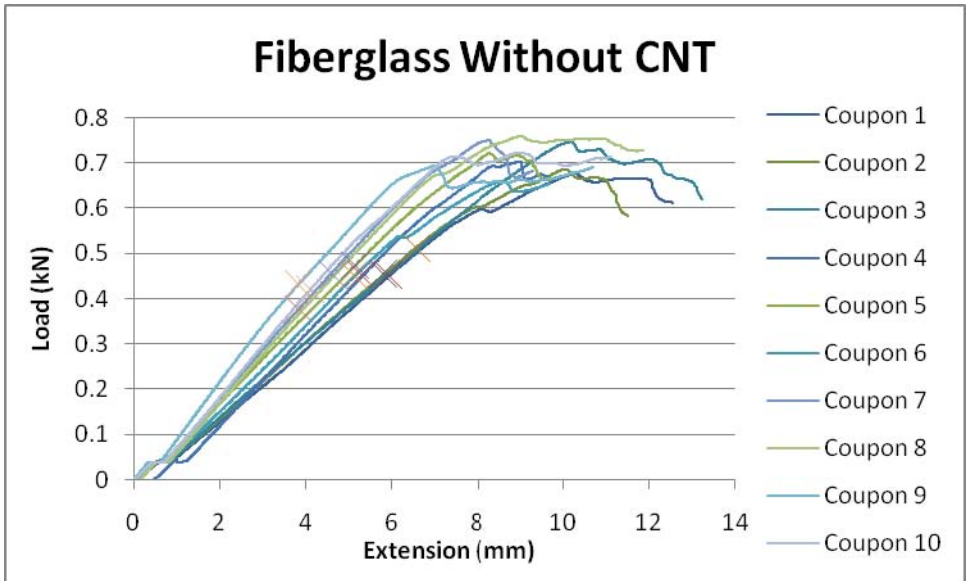

Figure 38. Mode II Graph of Fiberglass Composites Without CNT

Differences in both the sound of failure, and crack propagation can be directly contributed to the CNTs. In the non-reinforced samples, crack propagation began at the tip of the initial crack, and continued to propagate through the joint interface, as shown in

Figures 39 and 40. This crack occurred early in the loading cycle and slowly propagated while still maintaining an increasing load. For the fiberglass composites reinforced with CNTS they too initially propagated from the crack tip through the joint interface, however, at a certain point the crack took the path of least resistance under the layer of CNTs, as shown in Figures 41 and 42. This result was widely observed in the CNT reinforced samples, and is the reason for the loud crack sound heard.

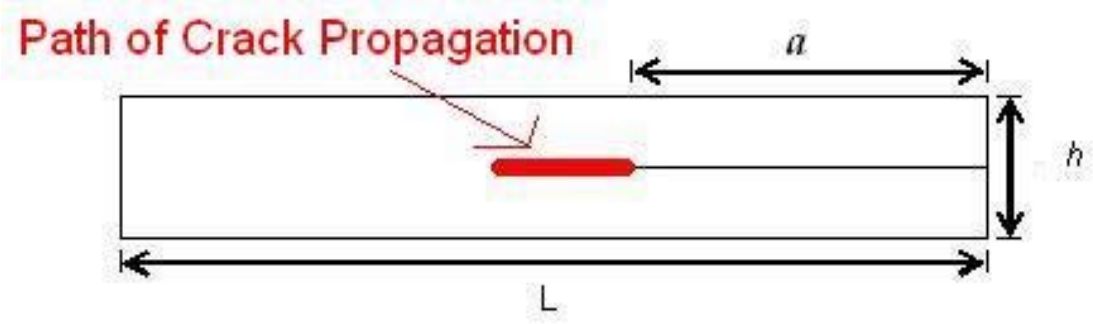

Figure 39. Fiberglass Composites Without CNT Path of Crack Propagation Drawing

Figure 40. Fiberglass Composites Without CNT Path of Crack Propagation Picture

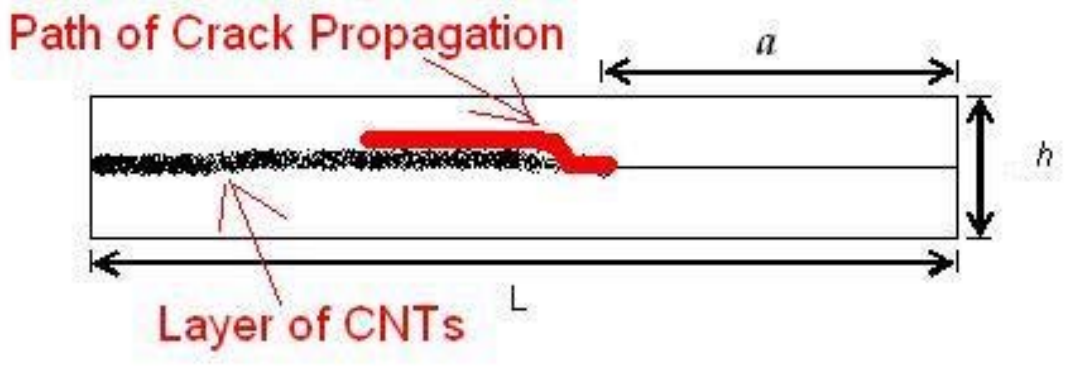

Figure 41. Fiberglass Composites With CNT Path of Crack Propagation

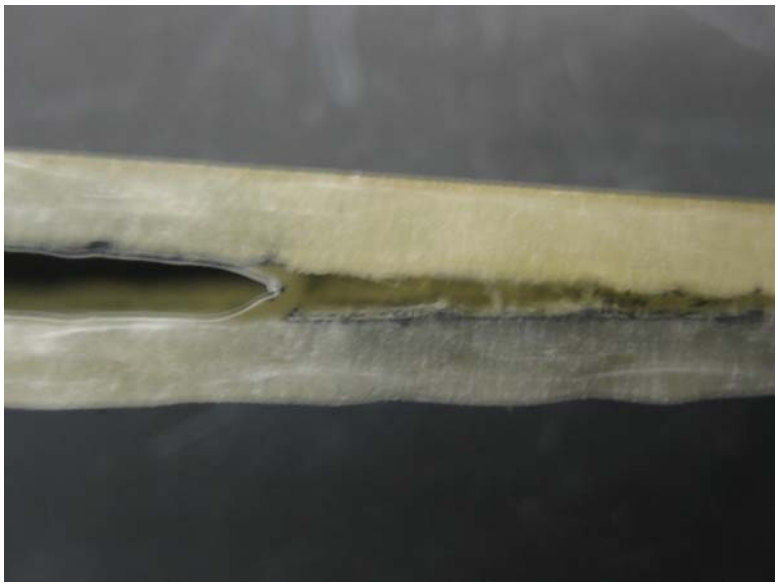

Figure 42. Fiberglass Composites With CNT Path of Crack Propagation Picture

After testing was complete for all phases of research, coupons in which crack propagation occurred were pulled apart to inspect the cracked joint interface surface, and verify crack propagation paths. When the fiberglass coupon with CNTs was pulled apart, one side contained more CNTs than the other. Looking closer it could be seen that initially the crack did propagate through the layer of CNTs, but then quickly took the path of least resistance under the layer of CNTs through the fiberglass. The fiberglass coupon without CNTs showed a slightly different crack propagation path. The joint interface

bond was broken through the resin by the crack propagation resulting in the resin being pulled away from the fibers. Both surface interfaces are shown below in Figures 43 and 44.

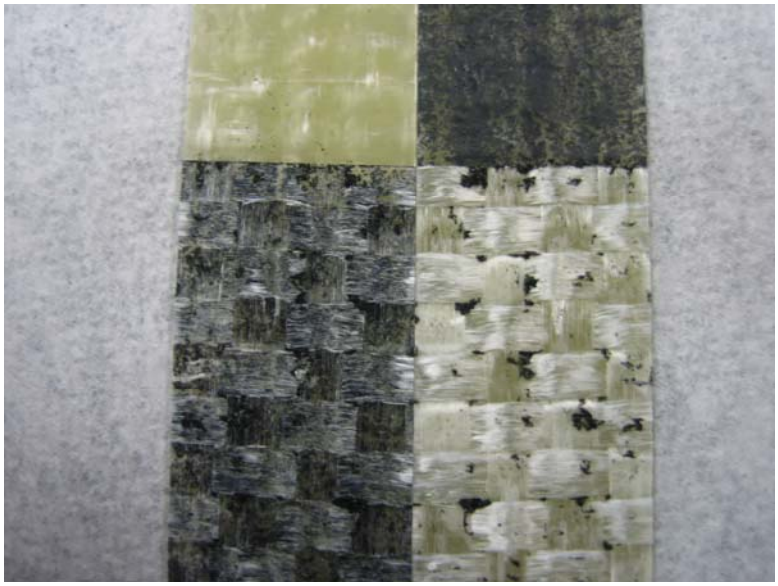

Figure 43. Surface Crack Propagation Path of Fiberglass Composite With CNT

Figure 44. Surface Crack Propagation Path of Fiberglass Composite Without CNT

The variances in surfaces can also explain the differences in both the physical observations, as well as the differences in the loads each sample set was able to carry.

The pure fiberglass composite acted as the two-step cured samples tested during Phase II. The crack propagated through the joint interface, an area which was inherently stronger due the VARTM process. This allowed for higher loads to be carried and slower crack growth. The fiberglass with CNT acted more like the co-cured samples from Phase II. Once the crack propagated into layers above or below that of the CNTs, it was propagating through a weaker resin bond allowing faster crack propagation and lower loads to be carried. This is ultimately why, although crack propagation was prolonged in the fiberglass with CNTs, those without were still able to carry higher loads.

E. PHASE V: RESIS TANCE RE LIABILITY AND CRACK GROWTH RELATIONSHIP TESTING

This phase began with testing of the four fiberglass composite coupons containing CNTs, from Phase IV, that resistance readings were able to be obtained. All coupons tested were placed on the Instron with the same test setup from Phase III and IV. In other words a span length of 16 cm, and width of 2.4 cm were still used. Before placing the coupons into the machine however, the length of the crack resulting from Phase IV Mode II tests were measured and recorded. Once loaded into the Instron, a load of 100 kN was applied to the coupons so that the crack was stationary without growth and the corresponding resistance readings were taken for both bent and unbent readings. This was done at least three times for each sample. The resulting resistance readings can be seen in Appendix G.

Although the readings vary from the cracked resistance readings taken in Phase IV, shown in Appendix E, each coupon is consistent within itself, only varying by at most 6.35%. Again the difference between the different coupons can be attributed to the uneven distribution of CNTs within the coupons. The readings also vary from that taken in Phase IV due to the different placement of where the multi-meter is attached on the sample. If this practice is to be used, the exact location of the test equipment placement must be marked in order to ensure consistent readings from one test to the next.

After taking the consistency readings, the fiberglass coupons were then manually loaded for crack growth using the Instron machine. Unfortunately, no useful information

was gathered from this step. Upon crack propagation, resistance readings jumped to over 1 MΩ. These high readings were indications that the CNTs were no longer touching and the sample was now acting as an open circuit. In essence, the crack had severed the continuous layer of CNTs and began to propagate below the layer of CNTs. This is what was observed and discussed in the Phase IV results when the samples were pulled apart for inspection.

The same two tests were then conducted using all carbon composite coupons containing CNTs, from Phase III. The same geometry setup was used, and the length of the crack resulting from Phase III Mode II tests was measured and recorded. This time a load of 50 kN was applied to the coupons, as 100 kN may have been a cause of the quick crack propagation experienced with the fiberglass coupon number four. The corresponding resistance readings for both the bent and unbent positions were taken. This was done at least three times for each sample. The resulting resistance readings can be seen in Appendix H.

As with the fiberglass composites, the readings for the carbon composites were consistent with each other. The average change in resistance was 1.26% with the highest resistance change being 8.77%. Any difference between the coupons can be attributed to the uneven distribution of CNTs within the coupons. As was seen with the fiberglass, the carbon readings also varied from those taken in Phase III. As already discussed, this is due to the different placement of where the multi-meter is attached on the sample.

After taking the consistency readings, the carbon coupons were then manually cracked using the Instron machine. Once the crack propagated, which was determined by both sight and sound, the new crack length was measured, and the corresponding resistance reading was taken. This was done repeatedly until the crack tip had reached the point of load application, and it was no longer possible to further crack the coupons with the Instron machine. The resulting data was then plotted to determine any relationship between change of crack length and change in resistance. Figure 45 shows all the data collected for coupons with CNT on one large graph.

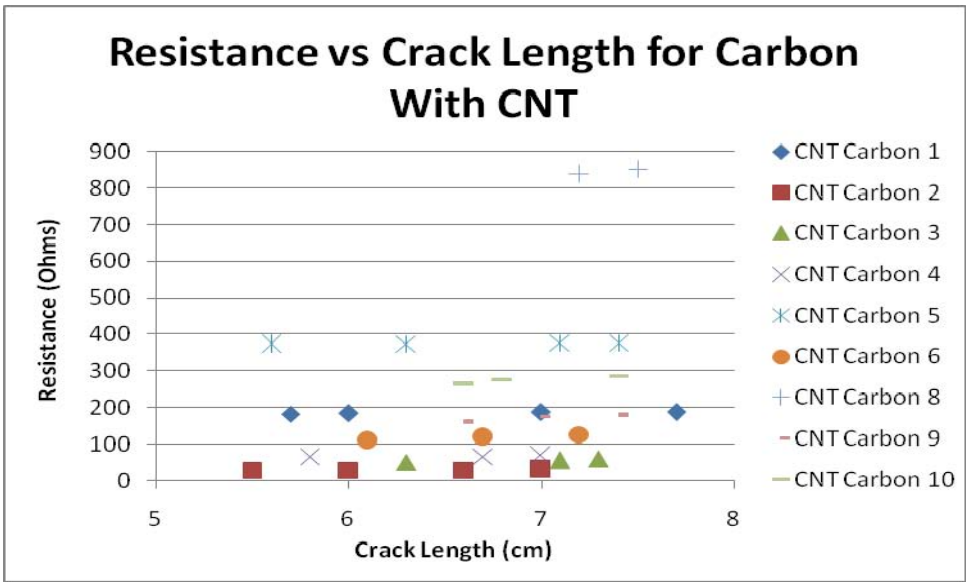

Figure 45. Carbon Composite Resistance vs. Crack Length Graph For All CNT Coupons

The above graph shows all the data minus the initial crack information. This was done to be more consistent in calculations. The resistance readings for the initial crack length of 4 cm were taken using a different test equipment position for the multi-meter, and therefore were not valid for these calculations. Unfortunately, even with these readings removed from the graph the data was still verily spread apart. This again is due to the uneven dispersion of CNTs in each of the coupons.

In an attempt to find some relationship between changes of crack length to changes of resistance, each coupon's data was plotted on its own graph. Most of the data followed a linear behavior, and so a linear regression was performed for each plot as shown in Figures 46, 47, 48, 49, 50, 51, 52, 53, and 54. These figures show that no standard slope could be found but an average was taken to be 13.68 Ohms/mm with a standard deviation of 14.52 Ohms/mm.

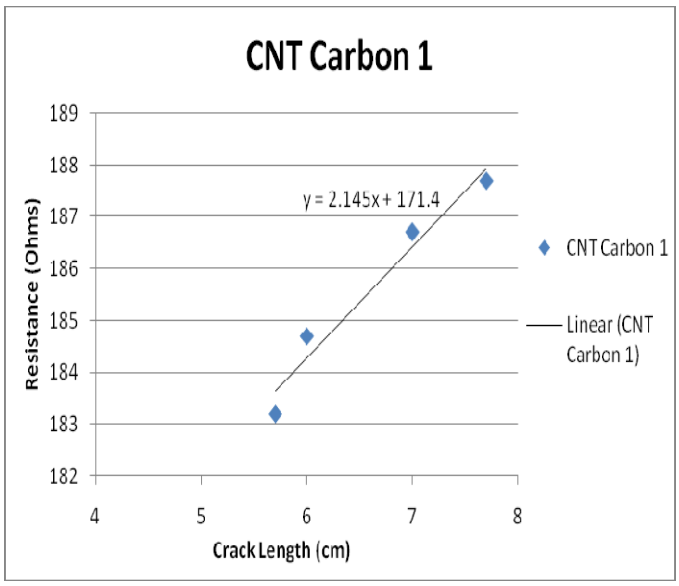

Figure 46. Carbon Composite Coupon 1 Resistance vs. Crack Length Graph

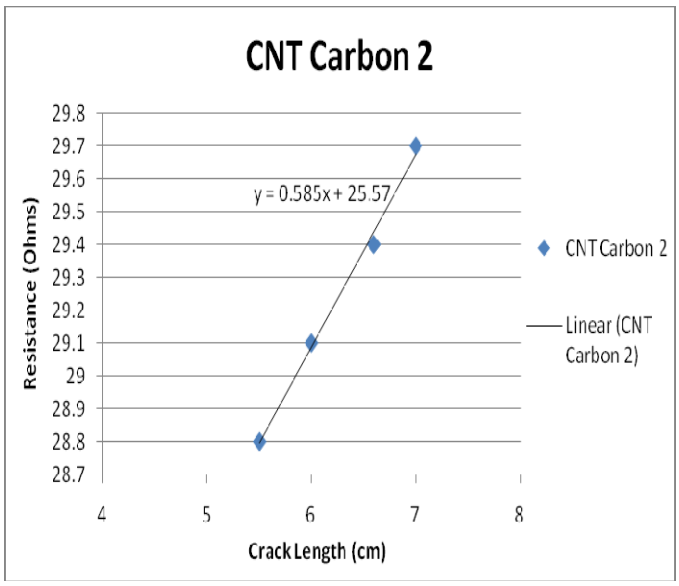

Figure 47. Carbon Composite Coupon 2 Resistance vs. Crack Length Graph

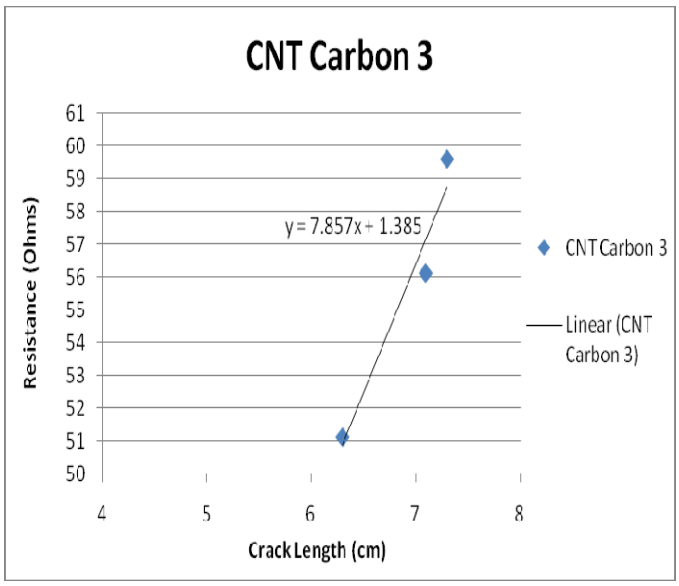

Figure 48. Carbon Composite Coupon 3 Resistance vs. Crack Length Graph

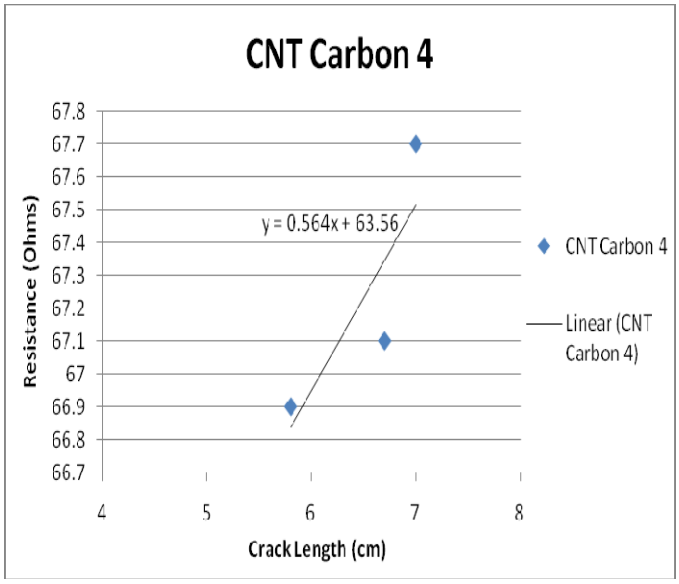

Figure 49. Carbon Composite Coupon 4 Resistance vs. Crack Length Graph

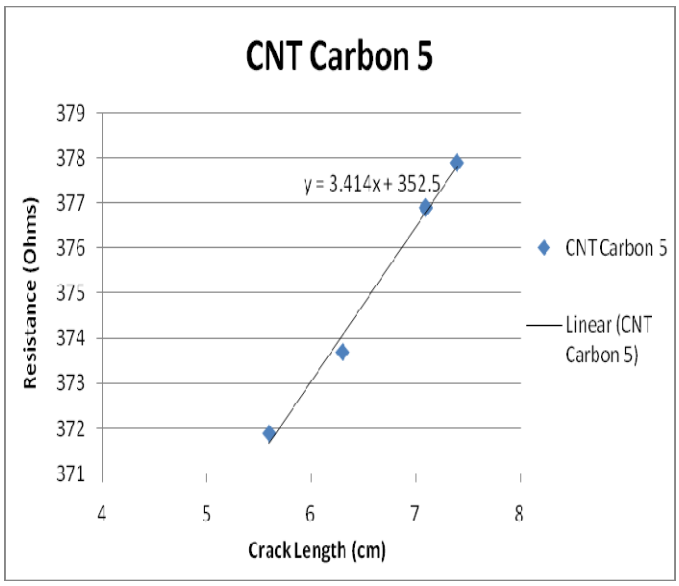

Figure 50. Carbon Composite Coupon 5 Resistance vs. Crack Length Graph

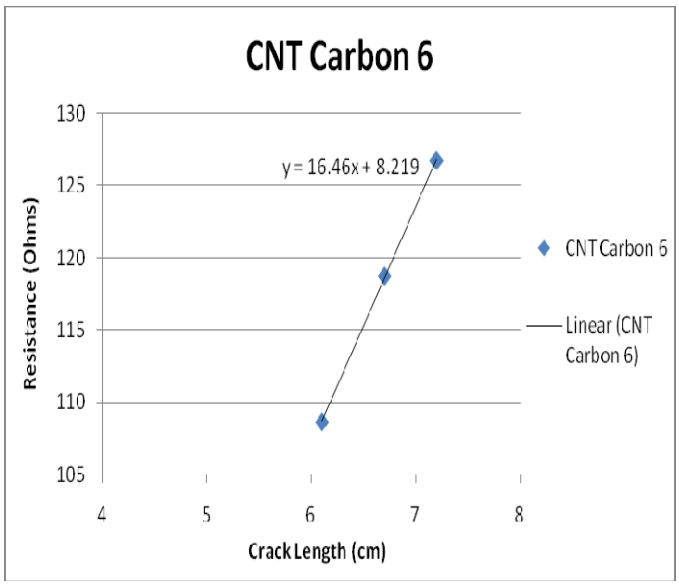

Figure 51. Carbon Composite Coupon 6 Resistance vs. Crack Length Graph

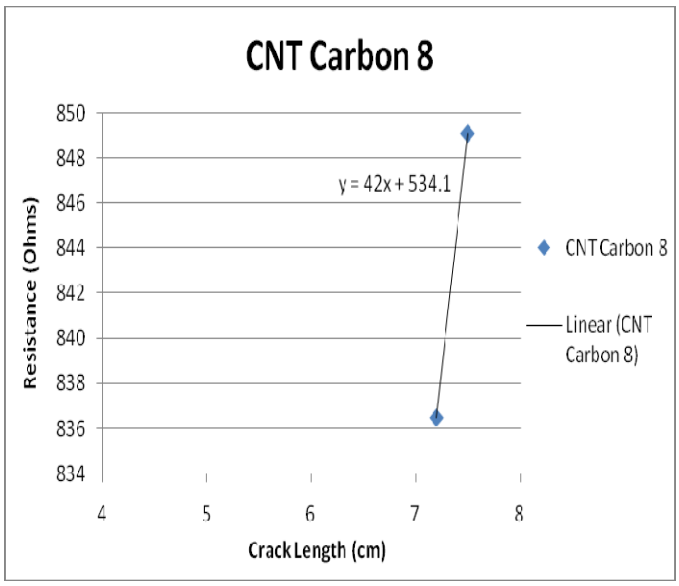

Figure 52. Carbon Composite Coupon 8 Resistance vs. Crack Length Graph

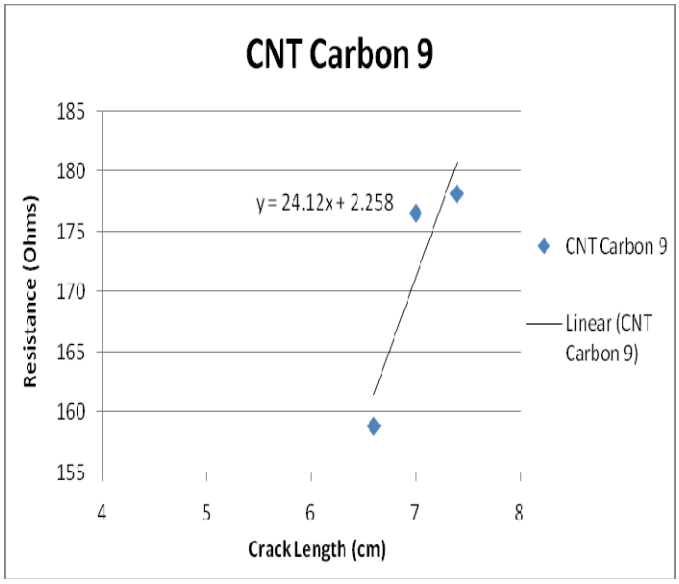

Figure 53. Carbon Composite Coupon 9 Resistance vs. Crack Length Graph

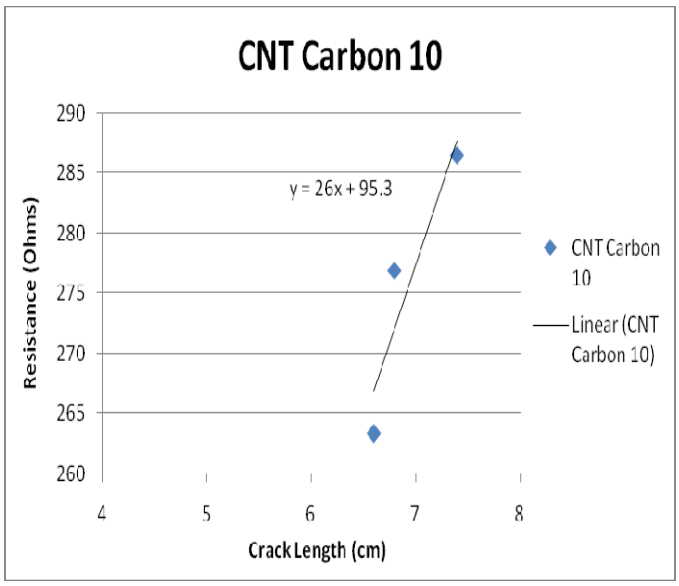

Figure 54. Carbon Composite Coupon 10 Resistance vs. Crack Length Graph

These figures all have the same general trends no matter what the starting crack length and initial resistance reading. With each incremental increase in crack length, the resistance values increased. Although it was difficult to predict how much the crack would propagate each time it was loaded, the resistance never failed to increase, even with the smallest increase in crack length. This increase in resistance is related to the fact that the crack for a carbon composite with CNTs propagates through the layer of CNTs. Thus, as the crack continues to propagate, the CNTs are separated from each other, and their ability to conduct throughout the sample is decreased. The more holes in the layer of CNTs, the harder it is to conduct, and thus an increase in resistance.

Although there seems to be a linear relationship, more testing needs to be done to verify these findings. More data points need to be taken in order to truly determine if a linear relationship is the correct one to assign to the resistance behavior of CNTs in composite materials. For future work this data could be improved by ensuring even dispersion of CNTs, designated test equipment positions for multi-meter, and a more scientific method to predict crack propagation in intermediate steps.

VI. CONCLUSIONS AND RECOMMENDATIONS

In conclusion, interface strength of woven fabric composite layers was studied using Mode II fracture mechanics testing. Both carbon fiber and glass fiber composites were used with the vinyl ester resin. Five phase of research were conducted, each looking at different aspects of the interface strength of composite layers. First, the co-cured composite interface strength was compared to that of the two-step cured interface as used in the scarf joint technique. The test results showed that the two-step cured interface was as strong as the co-cured interface, and the former had even higher fracture toughness than the latter. The conclusion is that the two-step cured interface is slightly better than the co-cured in terms of fracture toughness, however in terms of labor intensiveness, co-cure would be simply preferable.

The second study applied carbon nanotubes to the composite interface using the two-step cured technique. Mode II fracture testing was performed for the interface containing CNTs. The results indicated a great improvement of the interface fracture toughness due to CNTs for both carbon and fiberglass composites.

Finally, a study was conducted to detect interface crack growth using the CNTs introduced at the interface. Because CNTs have high electric conductivity, the electric resistance was measured through the interface. For fiberglass composites, due to their unusual paths of crack propagation, only the initial failure was detected through resistance. Carbon composites however, as the interface crack grew under loading, a gradual increase of electric resistance was observed upon unloading. As a result, the change of electric resistance in terms of crack length change was studied for carbon composite materials. Unfortunately, due to uneven dispersion techniques, and other testing procedures, it could only be determined that a linear relationship exists for these carbon composite materials. The study did show that using CNTs in carbon composite materials at a critical composite interface would not only strengthen its fracture toughness, but also detect crack growth.

Further research is necessary to verify the above findings and conclusions. Tests already conducted should be run again at different levels of CNTs concentrations, as well as with a better CNTs dispersion method. This will lead to closer resistance readings from coupon to coupon, and a more accurate crack length change to resistance relationship. When conducting any resistance tests, exact locations for test equipment, mainly the multi-meter clips, should be marked and used for all tests.

Furthermore, Mode I tests and Mixed Mode I-Mode II tests should be conducted while measuring the conductivity of composite materials. In actual structures, the stress will rarely be purely Mode II, and so all possibilities must be fully studied. Further research is also needed to determine feasible manufacturing practices for local CNT dispersion.

APPENDIX A: TWO-STEP CURED AND CO-CURED CRITICAL STRAIN ENERGY RELEASE RATES (G_{II})

Two-Step Cured

Sample	G_{IIC} (N/m)	C (m/N)	P_c (N)	L (cm)	a (cm)	b (cm)
2D	1.016E+03	9.4697E-06	713.901	6.5	2.6	2.40
2E	9.533E+02	8.6957E-06	721.556	6.5	2.6	2.40
2G	6.521E+02	6.7340E-06	608.57	6.0	2.6	2.40
2H	7.168E+02	7.0771E-06	643.331	6.0	2.5	2.40
2I	6.745E+02	9.2507E-06	545.831	6.0	2.5	2.40

Co-Cured

Sample	G_{IIC} (N/m)	C (m/N)	P_c (N)	L (cm)	a (cm)	b (cm)
1C	8.905E+02	1.0905E-05	584.557	6.5	2.8	2.40
1D	8.741E+02	1.1186E-05	589.716	6.5	2.7	2.40
1E	8.850E+02	1.1236E-05	592.069	6.5	2.7	2.40
1F	5.933E+02	9.0909E-06	534.883	6.0	2.4	2.40
1G	6.372E+02	9.2851E-06	512.308	6.0	2.6	2.40
1H	7.500E+02	9.7182E-06	511.263	6.0	2.8	2.40

THIS PAGE INTENTIONALLY LEFT BLANK

APPENDIX B: CARBON COMPOSITE WITH CNT RESISTANCE DATA PHASE III

Sample Number	Initial Resistance (Ohms)	Average Resistance During Testing (Ohms)	Resistance in Bent Position (Ohms)	Resistance in Flat Position (Ohms)	Percent Increase in Resistance
1	173.3	173.1	173.5	182.2	5.14%
2	26.5	26.5	26.9	28.1	6.04%
3	49.3	49.2	49.2	51.2	3.85%
4	71.6	71.6	71.1	73.1	2.09%
5	232.5	234.9	235.2	241.4	3.83%
6	287.2	286.4	277.6	293.1	2.05%
7	74.5	85.2	75.2	123.4	65.64%
8	1081.0	1043.5	1046.0	1112.0	2.87%
9	455.6	281.1	148.5	622.8	36.70%
10	252.5	300.1	288.8	326.2	29.19%
Group Averages	**270.4**	**255.2**	**239.2**	**305.4**	**15.7%**

THIS PAGE INTENTIONALLY LEFT BLANK

APPENDIX C: PURE CARBON COMPOSITE RESISTANCE DATA PHASE III

Sample Number	Initial Resistance (Ohms)	Average Resistance During Testing (Ohms)	Resistance in Bent Position (Ohms)	Resistance in Flat Position (Ohms)	Percent Increase in Resistance
1	91.25	25.93	16.61	76.60	-16.05%
2	9.16	4.27	3.67	6.23	-31.99%
3	1750.00	322.15	8.75	5500.00	214.29%
4	9.73	7.50	7.94	9.82	0.92%
5	18.10	10.64	5.05	18.10	0.00%
6	35.30	9.71	10.80	38.40	8.78%
7	453.00	8.82	5.21	71.30	-84.26%
8	435.20	58.56	4.30	454.00	4.32%
9	230.00	6.37	4.55	59.50	-74.13%
10	17900.00	23.00	7.25	1270.00	-92.91%
Group Averages	**2093.17**	**47.69**	**7.41**	**750.40**	**-7.10%**

THIS PAGE INTENTIONALLY LEFT BLANK

APPENDIX D: CARBON COMPOSITE WITH AND WITHOUT CNT CRITICAL STRAIN ENERGY RELEASE RATES (G_{II})

With CNT

Sample	G_{IIC} (N/m)	C (m/N)	P_c (N)	L (cm)	a (cm)	b (cm)
1	1.069E+03	1.8797E-05	480.229	8.0	4.0	2.40
2	1.161E+03	1.7953E-05	512.076	8.0	4.0	2.40
3	1.056E+03	1.6129E-05	515.066	8.0	4.0	2.40
4	1.103E+03	1.5898E-05	530.225	8.0	4.0	2.40
5	1.208E+03	1.9084E-05	506.515	8.0	4.0	2.40
6	1.023E+03	1.5361E-05	519.672	8.0	4.0	2.40
7	1.272E+03	1.7123E-05	548.763	8.0	4.0	2.40
8	9.998E+02	1.6835E-05	490.636	8.0	4.0	2.40
9	1.244E+03	1.7483E-05	537.113	8.0	4.0	2.40
10	1.116E+03	1.6367E-05	525.651	8.0	4.0	2.40

Without CNT

Sample	G_{IIC} (N/m)	C (m/N)	P_c (N)	L (cm)	a (cm)	b (cm)
3	8.392E+02	1.8519E-05	395.551	7.5	4.0	2.40
4	8.207E+02	1.6892E-05	409.557	7.5	4.0	2.40
5	9.486E+02	1.6313E-05	448.06	7.5	4.0	2.40
6	1.045E+03	1.6892E-05	462.116	7.5	4.0	2.40
7	7.502E+02	1.8692E-05	372.25	7.5	4.0	2.40
8	9.106E+02	1.9920E-05	397.264	7.5	4.0	2.40
9	1.042E+03	1.7483E-05	453.597	7.5	4.0	2.40
10	8.431E+02	1.5504E-05	433.296	7.5	4.0	2.40

THIS PAGE INTENTIONALLY LEFT BLANK

APPENDIX E: FIBERGLASS COMPOSITE WITH CNT RESISTANCE DATA PHASE IV

Sample Number	Initial Resistance (Ohms)	Average Resistance During Testing (Ohms)	Resistance in Bent Position (Ohms)	Resistance in Flat Position (Ohms)	Percent Increase in Resistance
1	38,120	38,572	39,950	44,550	16.87%
2	357,100	336,850	404,100	455,300	27.50%
4	73,090	74,531	88,100	146,500	100.44%
7	717,600	742,434	939,200	909,200	26.70%
Group Averages	**296,477**	**298,096**	**367,837**	**388,887**	**42.9%**

THIS PAGE INTENTIONALLY LEFT BLANK

APPENDIX F: FIBERGLASS COMPOSITE WITH AND WITHOUT CNT CRITICAL STRAIN ENERGY RELEASE RATES (G_{II})

With CNT

Sample	G_{IIC} (N/m)	C (m/N)	P_c (N)	L (cm)	a (cm)	b (cm)
1	9.803E+02	1.3106E-05	550.607	8.0	4.0	2.40
2	1.109E+03	1.2516E-05	599.307	8.0	4.0	2.40
4	1.054E+03	1.2063E-05	595.245	8.0	4.0	2.40
5	7.802E+02	1.3986E-05	475.502	8.0	4.0	2.40
6	9.257E+02	1.1148E-05	580.161	8.0	4.0	2.40
7	1.099E+03	1.2788E-05	590.156	8.0	4.0	2.40
8	1.084E+03	1.1481E-05	618.6	8.0	4.0	2.40
9	8.641E+02	1.2610E-05	527.009	8.0	4.0	2.40
10	8.978E+02	1.3986E-05	510.099	8.0	4.0	2.40

Without CNT

Sample	G_{IIC} (N/m)	C (m/N)	P_c (N)	L (cm)	a (cm)	b (cm)
1	6.181E+02	1.2315E-05	451.026	8.0	4.0	2.40
2	6.142E+02	1.2121E-05	453.201	8.0	4.0	2.40
3	7.960E+02	1.2392E-05	510.283	8.0	4.0	2.40
4	5.929E+02	1.0091E-05	450.409	7.5	4.0	2.40
5	6.796E+02	1.0395E-05	475.106	7.5	4.0	2.40
6	6.245E+02	1.0604E-05	450.901	7.5	4.0	2.40
7	4.611E+02	9.4162E-06	378.589	7.0	4.0	2.40
8	6.594E+02	9.4877E-06	451.02	7.0	4.0	2.40
9	6.475E+02	8.6505E-06	430.048	6.5	4.0	2.40
10	6.594E+02	9.2081E-06	420.631	6.5	4.0	2.40

THIS PAGE INTENTIONALLY LEFT BLANK

APPENDIX G: FIBERGLASS COMPOSITE WITH CNT RESISTANCE DATA PHASE V

Each coupon was tested at least three times using the following procedure.

1) Measure the crack length and initial resistance reading

2) Load and unload the coupon allowing no crack to propagate

3) Measure the resulting resistance reading

Each of the rows below represents the different trial runs for each sample.

Coupon 1:

New Crack Length (cm)	Initial Resistance Reading (ohms)	Load (N)	Final Resistance Reading (ohms)	Percentage Change
6.4	44300	100	44500	0.45%
6.4	44500	100	44600	0.22%
6.4	44600	100	44700	0.22%

Average: 0.30%

Coupon 2:

New Crack Length (cm)	Initial Resistance Reading (ohms)	Load (N)	Final Resistance Reading (ohms)	Percentage Change
6.2	771100	100	820100	6.35%
6.2	739000	100	739200	0.03%
6.2	739200	100	709000	4.09%

Average: 3.49%

Coupon 4:

New Crack Length (cm)	Initial Resistance Reading (ohms)	Load (N)	Final Resistance Reading (ohms)
6.5	285500	100	over 1 MΩ

Coupon 7:

New Crack Length (cm)	Initial Resistance Reading (ohms)	Load (N)	Final Resistance Reading (ohms)	Percentage Change
6	912600	100	891200	2.34%
6	914400	100	908200	0.68%
6	904600	100	871100	3.70%

Average: **2.24%**

APPENDIX H: CARBON COMPOSITE WITH CNT RESISTANCE DATA PHASE V

Each coupon was tested at least three times using the following procedure.

1) Measure the crack length and initial resistance reading

2) Load and unload the coupon allowing no crack to propagate

3) Measure the resulting resistance reading

Each of the rows below represents the different trial runs for each sample.

Coupon 1:

New Crack Length (cm)	Initial Resistance Reading (ohms)	Load (N)	Final Resistance Reading (ohms)	Percentage Change
5.7	182.1	50	182.3	0.11%
5.7	180.8	50	181.8	0.55%
5.7	181.5	50	181.9	0.22%

Average: 0.29%

Coupon 2:

New Crack Length (cm)	Initial Resistance Reading (ohms)	Load (N)	Final Resistance Reading (ohms)	Percentage Change
5.5	28.9	50	28.8	0.35%
5.5	28.8	50	28.7	0.35%
5.5	28.8	50	28.9	0.35%

Average: 0.35%

Coupon 3:

New Crack Length (cm)	Initial Resistance Reading (ohms)	Load (N)	Final Resistance Reading (ohms)	Percentage Change
6.3	51.3	50	51.7	0.78%
6.3	50.5	50	51.6	2.18%
6.3	51.2	50	51.6	0.78%
6.3	51.2	50	51.5	0.59%

Average: 1.08%

Coupon 4:

New Crack Length (cm)	Initial Resistance Reading (ohms)	Load (N)	Final Resistance Reading (ohms)	Percentage Change
5.8	67.2	50	67	0.30%
5.8	67	50	66.9	0.15%
5.8	67	50	67.1	0.15%

Average: 0.20%

Coupon 5:

New Crack Length (cm)	Initial Resistance Reading (ohms)	Load (N)	Final Resistance Reading (ohms)	Percentage Change
5.6	365.1	50	370.1	1.37%
5.6	372.2	50	371.1	0.30%
5.6	370.1	50	371.4	0.35%

Average: 0.67%

Coupon 6:

New Crack Length (cm)	Initial Resistance Reading (ohms)	Load (N)	Final Resistance Reading (ohms)	Percentage Change
6.1	93.5	50	101.7	8.77%
6.1	108.4	50	108.6	0.18%
6.1	99.4	50	103.2	3.82%

Average: 4.26%

Coupon 8:

New Crack Length (cm)	Initial Resistance Reading (ohms)	Load (N)	Final Resistance Reading (ohms)	Percentage Change
7.2	839.2	50	836.7	0.30%
7.2	840.1	50	846	0.70%
7.2	847.7	50	847.7	0.00%

Average: 0.33%

Coupon 9:

New Crack Length (cm)	Initial Resistance Reading (ohms)	Load (N)	Final Resistance Reading (ohms)	Percentage Change
6.6	157.7	50	163	3.36%
6.6	161.2	50	159.1	1.30%
6.6	160.5	50	160.5	0.00%

Average: 1.55%

Coupon 10:

New Crack Length (cm)	Initial Resistance Reading (ohms)	Load (N)	Final Resistance Reading (ohms)	Percentage Change
6.6	276.5	50	278.1	0.58%
6.6	276.1	50	276.6	0.18%
6.6	276.6	50	256.6	7.23%

Average: 2.66%

THIS PAGE INTENTIONALLY LEFT BLANK

LIST OF REFERENCES

Callister, William D., Jr. *Materials Science and Engineering: An Introduction*, 7th ed., New York: John Wiley and Sons, Inc, 2007.

Chou, Tsu-Wei and Erik T. Thosetenson. Carbon Nanotube/Vinyl Ester Nanocomposites for in Situ Sensing. September 17–19, 2008. University of Maryland University College, Adelphia, MD. *Office of Naval Research Solid Mechanics Program Review Meeting: Marine Composites and Sandwich Structures*.

Dharap, P., Z. Li, S. Nagarajaiah, and E.V. Barrera. 2004. Nanotube film based on single-wall carbon nanotubes for strain sensing. *Nanotechnology* 15.

Faulkner, Susan. "Study of Composite Joint Strength with Carbon Nanotube Reinforcement," Master's thesis, Naval Postgraduate School, 2008.

Harris, P.J.F. 2004. Carbon Nanotube Composites. *International Materials Review* 49.

Kang, I., M. J. Schulz, J. H. Kim, V. Shanov, and Shi, D. 2006. A carbon nanotube strain sensor for structural health monitoring. *Smart Materials and Structures* 15.

Kwon, Y. W., R. Slaff, S. Bartlett, and T. Greene. 2008. Enhancement of Composite Scarf Joint Interface Strength through Carbon Nanotube Reinforcement. *Journal of Materials Science*.

Live Journal. Definition of a Nanotube. March 12, 2009. http://fullerenes.livejournal.com/ (accessed September, 9 2009).

Mouritz, A.P., E. Gellert, P. Burchill, and K. Challis. July 2001. Review of Advanced Composite Structures for Naval Ships and Submarines. *Composite Structures* 53.

Nofar, M., S.V. Hoa, and M.D. Pugh. 2009. Failure Detection and Monitoring in Polymer Matrix Composites Subjected to Static and Dynamic Loads Using Carbon Nanotube Networks. *Composites Science and Technology*.

Saito, R. and M. S. Dresselhaus. Physical Properties of Carbon Nanotubes. 1998. Imperial College Press.

The Venton Research Group. Development of Carbon Nanotube Modified Microelectrodes. n.d. http://www.faculty.virginia.edu/ventongroup/nanotube.html (accessed September 9, 2009).

Thostenson, E.T., and T.W. Chou. 2006. Carbon Nanotube Networks: Sensing of Distributed Strain and Damage for Life Prediction and Self Healing. *Advanced Materials* 18.

Todo, M., T. Nakamura, and K. Takahashi. 2000. Effects of Moisture Absorption on the Dynamic Interlaminar Fracture Toughness of Carbon/Epoxy Composites. *Journal of Composite Materials* 34.

Weber, I., and P. Schwartz. 2001. Monitoring Bending Fatigue In Carbon-Fibre/Epoxy Composite Strands: A Comparison Between Mechanical and Resistance Techniques. *Composites Science and Technology* 61.

Wong, M., M. Paramsothy, X.J. Xu, Y. Ren, S. Li, and K. Liao. December 2003. Physical Interactions at Carbon Nanotube-Polymer Interface. *Polymer* 44.

Zhang, W., V. Sakalkar, and N. Koratkar. 2007. In Situ Health Monitoring and Repair In Composites Using Carbon Nanotube Additives. *Applied Physiscs Letters* 91.

INITIAL DISTRIBUTION LIST

1. Defense Technical Information Center
   Ft. Belvoir, Virginia

2. Dudley Knox Library
   Naval Postgraduate School
   Monterey, California

3. Graduate School of Engineering and Applied Sciences
   Naval Postgraduate School
   Monterey, California

4. Joe Johnson
   Integrated Composites Inc.
   Marina, California

5. John Dickie
   Integrated Composites Inc.
   Marina, California

6. John McWaid
   Integrated Composites Inc.
   Marina, California

7. Ray Uncangco
   Integrated Composites Inc.
   Marina, California

8. Professor Young W. Kwon
   Naval Postgraduate School
   Monterey, California

9. Major Randall D Pollak
   Naval Postgraduate School
   Monterey, California

10. Professor and Chairman Knox T. Millsaps
    Naval Postgraduate School
    Monterey, California

11. Lieutenant Mollie A. Bily
    Naval Postgraduate School
    Monterey, California